Wetter climate favouring early Lapita horticulture in Remote Oceania

Giorgia Camperio[1,2*], S. Nemiah Ladd[3], Matiu Prebble[4,5], Ronald Lloren[1,2], Elena Argiriadis[6,7], Daniel B. Nelson[8], Christiane Krentscher[1], Nathalie Dubois[1,2]

*Corresponding author: giorgia.camperio@eawag.ch

Affiliations

[1]Department of Surface Waters Research & Management, Eawag, Dübendorf, 8600, Switzerland
[2]Department of Earth Sciences, ETH Zürich, Zürich, 8092, Switzerland
[3]Department of Environmental Sciences, University of Basel, Basel, 4056, Switzerland
[4]School of Earth and Environment, College of Science, University of Canterbury, Christchurch, 8041, New Zealand
[5]Archaeology and Natural History, Culture History and Languages, The Australian National University, Canberra, ACT 2010, Australia
[6]Institute of Polar Sciences, CNR-ISP, Venice, 30172, Italy
[7]Department of Environmental Sciences, Informatics and Statistics, Ca' Foscari University, Venice, 30172, Italy
[8]Department of Environmental Sciences – Botany, University of Basel, 4056, Basel, Switzerland

E-mail addresses:
giorgia.camperio@eawag.ch
n.ladd@unibas.ch
matiu.prebble@canterbury.ac.nz
Ronald.lloren@eawag.ch
elena.argi@unive.it
daniel.nelson@unibas.ch
christiane.krentscher@gmail.com
nathalie.dubois@eawag.ch

Wetter climate favouring early Lapita horticulture in Remote Oceania

Giorgia Camperio[1,2*], S. Nemiah Ladd[3], Matiu Prebble[4,5], Ronald Lloren[1,2], Elena Argiriadis[6,7], Daniel B. Nelson[8], Christiane Krentscher[1], Nathalie Dubois[1,2]

*Corresponding author: giorgia.camperio@eawag.ch

Affiliations

[1]Department of Surface Waters Research & Management, Eawag, Dübendorf, 8600, Switzerland

[2]Department of Earth Sciences, ETH Zürich, Zürich, 8092, Switzerland

[3]Department of Environmental Sciences, University of Basel, Basel, 4056, Switzerland

[4]School of Earth and Environment, College of Science, University of Canterbury, Christchurch, 8041, New Zealand

[5]Archaeology and Natural History, Culture History and Languages, The Australian National University, Canberra, ACT 2010, Australia

[6]Institute of Polar Sciences, CNR-ISP, Venice, 30172, Italy

[7]Department of Environmental Sciences, Informatics and Statistics, Ca' Foscari University, Venice, 30172, Italy

[8]Department of Environmental Sciences – Botany, University of Basel, 4056, Basel, Switzerland

Key words

Pacific seafarers, Paleoclimate, Sediment cores, Biomarkers, SPCZ

Abstract

The islands of Remote Oceania were among the last places on Earth colonised by humans. Lapita seafarers carrying with them an extensive root-tuber-tree crop complex and domestic animals, rapidly transformed nearly all of these previously unoccupied islands. However, the timing of initial Lapita settlements and the early introduction of horticulture remain a matter of debate as significant changes in climate coincided with human oceanic explorations in the mid-late Holocene. Here we show that fossil biomarkers preserved in sedimentary archives located near Teouma, the earliest dated Lapita cemetery in Remote Oceania, trace human presence and horticultural practices while providing the climatic context for the initial settlement. Using fossil faecal molecules, the hydrogen isotopic composition of leaf waxes, and palmitone, a molecular marker for the staple crop taro (*Colocasia esculenta* Schott), we identified signatures of human activity spanning the period of occupation recorded at the Teouma site. The temporal precision provided by our high-resolution radiocarbon chronology refines the settlement timing with a first unequivocal human trace appearing at 2739-2879 BP. The presence of taro in the initial settlement period attests to the early introduction and likely rapid expansion of horticulture by the first settlers. Lower leaf wax hydrogen isotope ratios starting approximately 2900 years ago further reveal that the initial settlement coincided with a transition to a wetter period, possibly driven by shifts of the South Pacific Convergence Zone. Our findings provide evidence of early horticulture in Remote Oceania and reveal the climatic context that favoured first human settlements in the islands.

Introduction

Remote Oceania, a region characterised by larger inter-island distances, extends from the eastern Solomon Islands to the Polynesian triangle of the Hawaiian Islands, Rapa Nui and Aotearoa/New Zealand[1] (Figure 1). These islands were on the oceanic pathways of multiple groups of horticulturalist seafarers throughout the last 3500 years. Early seafarers originated from Island Southeast Asia and Papua, while later migrations extended east to Polynesia[2–7]. The Lapita Cultural Complex, characterised by dentate-stamp ceramic ware, is associated with the earliest group to reach Remote Oceania[8–10] whose descendants became the foundational cultures for most of the Pacific Islands (Figure 1). It has been suggested that during particular periods, climate windows may have favoured certain human migration routes[11–13] with adverse climatic conditions inducing land abandonment[14] or migrations to new islands[15]. In addition, past precipitation changes could have played a role in settlement patterns by influencing cultivation practices[16,17], driving cultural adaptations[18,19] and leading to differing migration routes and timing[15]. However, few climatic records covering this time window have been produced in Remote Oceania, hindering efforts to determine the actual influence of climate on human settlement patterns.

The archipelago of Vanuatu contains extensive archaeological remains of the Lapita Cultural Complex, and is considered a key location in the initial settlement of Remote Oceania[20].

The islands of Vanuatu and archipelagos to the East were previously unoccupied prior to Lapita arrival (Figure 1). Exact dating of early sites in Vanuatu associated with the Lapita is often complicated by intense perturbations due to post-depositional disturbance, inbuilt age, and reservoir offsets[21,22]. Although U/Th dating of coral artefacts has been used for precise dating of early settlements in Tonga[23] there are no such dates available for Vanuatu, which lies in the Western root of the Lapita migration. In addition, despite significant improvements in radiocarbon techniques, these dates can still have large uncertainties, challenging a clear timeline of human settlement in the region[22,24]. Similarly, while there is evidence of early agricultural practices in Vanuatu, such as terraced gardens[25] and introduced crops[26–28], identifying the precise timing and extent of horticultural practices has been hindered by uncertainties in stratigraphy, dating, and biological proxies[29].

Given its archaeological importance for reconstructing the initial human settlement of Remote Oceania and its position at the south-western edges of the South Pacific Convergence Zone (SPCZ), Vanuatu is ideally located to improve our understanding of the role of past climatic drivers on ancient settlements and migrations. Changes in precipitation are the main local climatic variable and are influenced by the Western Pacific Warm Pool (WPWP) and the SPCZ[30], both interconnected to the Intertropical Convergence Zone (ITCZ)[31]. Given the strong precipitation gradients that characterise the SPCZ, any shifts in its location and intensity can have far-reaching implications for island communities[32]. Interannual climate variability is influenced by the El Niño-Southern Oscillation (ENSO), which alters both the WPWP and SPCZ, causing droughts during El Niño and wetter conditions during la Niña[33,34]. ENSO-driven climate patterns can have significant impacts on the availability of water resources and agricultural productivity[35] and may have affected early settlements.

Here, we track human arrival and hydroclimatic changes using lipid biomarkers from Emaotfer swamp sediments from the island of Efate, Vanuatu (Figure 1). Emaotfer swamp is located one kilometre east of Teouma, the earliest dated Lapita cemetery in Remote Oceania and one of the most important archaeological sites of the Lapita culture, providing evidence for much of what we know about their ancient food production, material culture, funerary practices and human genetic diversity[36,37]. We use faecal fossil molecules, namely coprostanol (5β-cholestan-3β-ol) and its epimer, epicoprostanol, as indicators of human presence. These molecules are produced by gut microbes as a metabolic product of cholesterol and are most abundant in human faeces[38] and have been used in archaeological context to reconstruct demographic changes[39,40]. Taro is the main staple crop of the region and its introduction by early settlers has been debated[41,42]. Standard taro cultivation practices prevent flowering and can limit pollen production, hindering identification of taro cultivation in sediments using traditional palynological analysis[43,44] (Prebble and Wilmshurst 2009; Prebble et al. 2019). We circumvent these issues using palmitone (hentriacontan-16-one), a unique taro (*Colocasia esculenta*) biomarker not linked to pollen production[45]. Finally, to understand the role of climate in the initial settlement of Remote Oceania and the establishment of horticulture, we use the compound specific hydrogen isotopic composition of leaf wax long chain *n*-alkanoic acids from higher plants. These reflect changes in precipitation[46] and can be used to reconstruct past hydroclimate in the tropical Pacific[47]. This study employs a multiproxy approach by combining climatic proxies and human markers within a sedimentary record spanning the last 5000 years.

The objective of this study is to track the first signs of human presence at the Teouma site and understand the role of climate on Lapita settlements and the onset of horticulture in Remote Oceania.

Results

Landscape dynamics

The archipelago of Vanuatu lies on the Pacific/Australian margin and is the result of emerged volcanic rocks and their interaction with Quaternary sea level changes and tectonic uplifts, resulting in exposed limestone terraces on most of the islands[48]. The Teouma archaeological site is located on an uplifted limestone reef which emerged approximately 4000 years ago[49], following uplift of the island but also coincident with the end of the mid-Holocene sea level highstand in the region[50].

Emaotfer sediments record this uplift as a transition from a marine lagoon to a freshwater environment at ca. 4000 BP (Before Present indicates calibrated years before 1950) (Figure 2).

The marine phase is identified by high $\delta^{15}N$ values (supplementary Figure S1) and high terrigenous element counts (supplementary Figure S2). The switch from a marine to lacustrine setting is supported by a decline in mangrove forest around the basin[51] and is associated with a transient peak in manganese (Mn) deposition (supplementary Figure S3), suggesting a shift in redox conditions and a sudden deposition of Mn.

These tectonic movements led to the emergence of new favourable land for first human settlement and the formation of a freshwater reservoir. The lacustrine phase lasts until the appearance of peat between 1792-2114 BP, characterised by lower values of the C/N ratio (mean 16 ± 2) and $\delta^{15}N$ (mean 0.9 ± 0.3). The lacustrine phase can be separated into two distinct intervals: An older one from 4000 BP to ca. 2900 BP, characterised by high values of terrestrial elements (Al, Fe, Ti), and a younger one from 2900 BP to 2000 BP, characterised by high values of the Ca/Al ratio (Figure 2). We attribute this change to the disconnection of the Teouma river from Emaotfer swamp (2811-2985 BP) (Supplementary Figure S4). The Teouma river is a meandering river currently flowing on the western side of the Teouma valley (Figure 1). The river disconnection is signalled by the drastic increase in the calcium to aluminum ratio (Ca/Al) linked with the final drop in terrigenous elements (Figure 2).

Three major drivers (or a combination thereof) can explain the discontinuation of the river water supply to the swamp. First, tectonic movements causing an uplift could have led to river avulsion prior to human arrival. As shown in Figure 1, Emaotfer swamp lies at the same altitude as the Teouma Graben. It is likely the course of the river once flowed to the northwest of our coring site. Second, the drying trend preceding this disconnection (Figure 3) could have lowered flow and prevented river waters from reaching the swamp. When conditions got wetter again, the river course would have been in a new location, as is typical of meandering rivers. Finally, water management for cultivation could explain the disconnection. Numerous examples of sophisticated and large-scale (multiple ha) irrigation and water management systems exist in the historic and archaeological record of Efate and neighbouring islands[52–55].

Molecular tracers of human occupation

The proximity of Emaotfer swamp to the Teouma site facilitates a detailed comparison with the archaeological findings and specifically with the settlement chronology based on radiocarbon dating of shells and human remains retrieved from the site[22,24]. The temporal precision provided by the sedimentary age model, derived from 40 radiocarbon dated samples (Figure 2), is key to capturing the short settlement history of the Lapita and provides a further constraint to the first period of human occupation of the Teouma site. High-resolution dating based on 26 samples provides a well-constrained age model between 2220 and 3860 cal yr BP, which includes the period of first human occupation (supplementary figure S5). Age reversals in the marine sediment phase, root intrusions, and hardwater effects (identified by higher $\delta^{13}C$ values of eight macrofossils, supplementary table 1) at the peat transition result in higher age uncertainties in these two phases.

Fossil molecules associated with human presence (faecal markers) and activities (palmitone) highlight three main periods of human occupation (Figures 2 and 4) starting ca. 2800 BP until present. The first period from 2739-2879 BP to 2624-2750 BP is a short period of occupation and is coincident with the first Lapita settlement at Teouma, which indeed would have only lasted a few generations[22]. The Bayesian chronological framework proposed by Petchey et al. [22] indicates 2870-2920 BP as the most likely start date of occupation of the site, but challenges related to cleaning, correction, and dietary considerations can limit the chronological precision of the available archaeological materials. We used radiocarbon dating of short-lived material deposited in the Emaotfer sedimentary basin to further constrain the site chronology with a first unequivocal human trace appearing at 2739-2879 BP, at the youngest limit of the age (2920–2870 BP) proposed by Petchey et al.[22].

Increases in TOC and TN at 2850 BP signify higher aquatic productivity (Figure 4), which is often a sign of human activities[56]. This is associated with a slight increase in Fe and Ti (Figure 2) and in sediment grain size (Figure 4), indicating a relative increase in erosion[57]. These sedimentary signatures also characterise subsequent periods of human presence and could be associated with land clearing and horticultural practices[25]. Indeed, the highest peak in palmitone, the biomarker associated with taro, the main staple crop of the region, coincides with this first period of human occupation (Figure 2). Such a strong signal can be the result of early extensive and intensive taro cultivation, and possibly from a direct establishment of taro gardens on the shore of Emaotfer swamp. Previous studies of the Lapita diet have demonstrated a ~~primary~~ reliance on marine resources[58,59]. However, the early introduction of taro as part of a "transported landscape" has long been hypothesised for the Pacific Islands[60]. Previous linguistic and archaeological studies have associated the introduction of taro with first settlements[41]. In our record the coincidence of the first peak in palmitone and in faecal markers explicitly signal the introduction and cultivation of taro by first Lapita settlers.

A second period of human occupation is evident in the core with a second peak in palmitone and faecal markers between 2400-2602 BP and 2298-2477 BP and follows after ca. 250 years of what could be a demographic decrease or even an absence of humans. Archaeological[49], anthropological[58,61] and ancient DNA studies have revealed two distinct phases of human occupation of the Teouma site[3,62]. The biomarker record supports a subsequent separate settlement, which coincides with the Erueti period, identified by a 50 cm midden deposit that covered the Lapita cemetery at the Teouma site at ca. 2400 BP[49]. The Erueti period is characterised by substantial changes in pottery style, mortuary practice, and in diet[49,58,59,61].

After 2300 BP no further archaeological traces of human occupation were found at the Teouma site, which appears to have been abandoned until the development of a coconut plantation in the early 20th century[49]. However, it should be noted that in such a geodynamic context (sea level, uplift, earthquakes, etc.) signs of human occupation might be lost[63]. In our record, there are signs of a pause in human occupation after 2500 BP but an increase in faecal markers and palmitone is evident around 2000 BP, a time devoid of archaeological traces at the Teouma site[49]. The swamp sediment is likely incorporating material from a larger catchment area than what is preserved at the archaeological site. The biomarkers related to human presence and activity remain high from 2000 BP on, with some variations, indicating continuous human occupation of the island. The Mangaasi archaeological site northwest of Efate (Figure 1) attests the presence of humans on the island ca. 2500-1200 BP[64]. During the last millennium, a demographic increase is evident from the widespread landscape features associated with cultivation and settlements that were observed by lidar imaging[52], which are coherent with the highest peaks in faecal markers ca. 1000 BP observed in the core. This demographic increase could be associated with the Roi Mata's Domain, considered a period of unity and prosperity on the island[65] which is traced archaeologically in the small near-shore island of Artok northwest of Efate (Figure 1).

Late Holocene SPCZ shifts

The hydrogen isotopic composition (δ^2H) of *n*-alkanoic acids was measured in 91 samples to identify past changes in precipitation[47] (Figure 3). First human traces were detected in the middle of a climatic shift towards significantly wetter conditions, which started ca. 2781-2964 BP, a few decades to a century before the first signs of humans in the sediment record (2739-2879 BP). The abrupt increase in precipitation is part of a general pattern observed in the core, where stepwise shifts towards wetter conditions (10-20 ‰) were recorded at 3600 BP, 3300 BP, 2900 BP, and at 2200 BP, just before the appearance of the peat at 2000 BP (Figure 3). The general trend towards wetter conditions was interrupted by drier and stable periods lasting a few centuries except for the period between 2600 BP and 2200 BP characterised by greater fluctuations.

Changes in precipitation on the island of Efate are determined by the SPCZ, which is in turn closely linked to both ITCZ and ENSO dynamics. Past changes in the SPCZ position remain poorly constrained[32,66]. However, an increase in precipitation lasting approximately 200 years between 2700-2200 BP inferred from ^{2}H-depleted nC26 in a sediment core from Sāmoa was associated with SPCZ expansion and a negative phase of the Interdecadal Pacific Oscillation[67]. An abrupt increase in sea surface temperature (SST) in the WPWP ca. 2800 BP could also have caused the wetter shift registered in our core[68], as higher SSTs are associated with increased precipitation from the SPCZ[69]. Model results suggest a southward and more variable position of the SPCZ in this period[34,70].

The SPCZ is a prominent extension of the ITCZ, yet how the SPCZ responded to changes in the ITCZ is not clear[32,70]. By comparing our climatic reconstruction of the SPCZ with ITCZ reconstructions, we could improve our understanding of the interaction between these climatic features. Paleoclimatic reconstructions available across the Pacific (Figure 3) indicate a southward migration of the ITCZ over the late Holocene[71–73]. A steady decrease in Ti% in the Cariaco Basin indicates a southward shift of the ITCZ[71] around 2850 BP, which could have had a role in the wetter trend recorded in Emaotfer core at that time. Seasonal increases in precipitation associated with the southward migration of the ITCZ are also recorded in the clay content of El Junco, in the Galapagos Islands[73]. Taking dating uncertainties into account, the two-step increase in precipitation observed at 3200 ±160 BP and 2000 ±100 BP in El Junco is also visible in Emaotfer record (Figure 3). On the Western side of the Pacific, a decrease in the Asian Summer Monsoon recorded in the $\delta^{18}O$ of stalagmites from the Dongge Cave of Southern China around 2800 BP is also connected with the southward movement of the ITCZ and highlights the interoceanic changes happening in that period[72].

ENSO influences the location of the SPCZ, although this dynamic is complex and can determine regional differences not ultimately linked with the various ENSO flavours[74,75]. An increase in ENSO frequency around 3000 BP is observed across the Pacific[76] and an associated drier trend starting at this time was recently described using carbon isotope ratios of leaves preserved in lake sediments from Western Australia with dry events associated with prolonged extreme El Niño events between 2600 and 2000 BP[77]. These drier trends are coherent with $\delta^{18}O$ measured in coral records from Papua New Guinea[78]. Increased frequency and amplitudes of El Niño between 2800 and 1500 BP are also recorded in the Galapagos[73,79]. An intensification of ENSO at 3000 BP would cause a drier climate on Efate. A direct one-to-one ENSO reconstructions require yearly resolved records, however in our record we do not observe an ENSO intensification starting at 3000 BP. Wirrmann et al.[80] report a change from rainforest to grass between 2800 BP and 2400 BP in a paleoecological study from Emaotfer swamp. They associate the change in vegetation to an intensification of ENSO but lower resolution and age uncertainties limit the use of their record for comparison. Most likely modern ENSO dynamics only started exerting a role on Efate ca. 2600 BP when increased δ^2H values indicate drier and more variable conditions, coincident with the extreme drying events recorded in Western Australia and Papua New Guinea[77,78].

Discussion

Our findings provide evidence of early horticulture in Remote Oceania and reveal the climatic context that favoured first human settlements in the islands. The 5000 year long sediment core from Emaotfer swamp is in high agreement with the archaeological record of the Teouma site, and the high resolution age constraints refine previous estimates of earliest possible use of the site. Our sediment core tracks the first human arrival at 2739-2879 BP, recorded as a peak in faecal markers, coincident with the establishment of horticulture signalled by the introduction of taro, recorded by increased palmitone accumulation.

First settlers arrived during a time of hydroclimatic change from a drier period to a wetter one, most likely linked with a southward shift of the ITCZ and expansion of the SPCZ. Emaotfer Swamp became disconnected from the Teouma River system right before the first human traces. Whether humans, climate or tectonics caused this disconnection remains an open question. The fossil molecule record confirms the influence of climate on human settlements in Remote Oceania. Climatic influences on human migrations and settlements have been described worldwide[81–86]. In the Pacific, climate has been suggested as a factor influencing navigation[11,12], horticultural expansion and as a possible explanation for the dietary differences observed between subsequent human groups, as the difference observed between the Lapita and the subsequent Erueti people[87].

The Emaotfer climatic record provides further context to the differences characterising the two archaeological phases of occupation at the Teouma site. Lower δ^2H values in the leaf wax record, indicative of a wetter climatic window from 2781-2964 BP until 2602-2713 BP, would have provided the ideal conditions for the establishment of horticulture during the Lapita period, as indicated by the highest concentration of palmitone, indicative of taro cultivation. The establishment and expansion of horticulture during the Lapita period would have relied on these favourable climatic conditions; the availability of water, along with fertile soils and cultivation management practices, could have contributed to successful horticultural establishment. Following previous reconstructions of climate windows for human migration in the Pacific[11,15], our climatic reconstruction of Emaotfer raises several questions. The drier period preceding the first human signal in the core may have played a role in triggering human migrations in search for new favourable settings or the end of the wetter period characterising their settlements could have contributed to site abandonment. The coeval Lapita settlement of Tonga[23] could indicate that similar drivers influenced the Lapita expansion further to the east.

The end of the brief wetter period, which favoured horticultural development, marks the end of the Lapita settlement at the site. A second peak in palmitone and faecal markers at 2400 BP corresponds with the Erueti phase observed in the archaeological records. The more variable and drier climate during the Erueti period is likely influenced by ENSO effects on the SPCZ. The drier conditions associated with the Erueti period may have contributed to a decline in human presence, as indicated by an abrupt decrease in the archaeological signal. The scarcity of resources and the challenges posed by drier environments could have influenced the decision to abandon or reduce occupation in certain areas. The lower palmitone signal during the Erueti period might also reflect the impact of drier climatic conditions on crop yields. The reduced availability of water or changes in precipitation patterns could have affected agricultural productivity, potentially leading to food scarcity or agricultural difficulties for the Erueti settlement. Despite some fluctuations in faecal markers and palmitone concentrations possibly related to demographic changes, biomarkers reveal that humans were present in the catchment until modern times.

The archaeological evidence found at various sites, including the Mangaasi site in the Northwest of the island (Figure 1), testify to human presence subsequent to the Lapita settlements, suggesting that the influence of climatic effects on past settlements was not consistent throughout. This indicates that different areas may have experienced varying degrees of impact from climate change.

Our findings provide evidence of early horticultural activities in Remote Oceania and demonstrate the importance of precipitation variability in determining both when humans settled remote islands, as well as the resource-acquisition strategies they employed upon arrival.

Material and methods

Study site

Emaotfer is a shallow swamp located on a limestone terrace 17 m above sea level on the southern coast of the Island of Efate. The swamp is located east of the Teouma Graben, into which the Teouma River flows (Figure 1). The water depth is influenced by seasonal changes in precipitation with a wet/cyclone season from November to April and a dry season from May to October. Annual rainfall is around 2100 mm but can vary strongly during El Niño (dry) and La Niña (wet) periods. Two paleoecological studies have previously reconstructed vegetational changes from Emaotfer swamp, but have not detected signals of human presence corresponding with the time of occupation of the Teouma site[51,80].

Coring and sub-sampling

In July 2017, we retrieved 3 cores from Emaotfer swamp using a standard Russian peat corer (lat. 17°47'6.66" S, long. 168°23'55.22" E). Water depth at the coring site was 0.3 m. The 50 cm core sections were wrapped twice in plastic foil, placed in halved PVC tubes, stored in a cooler and flown back to the Eawag laboratories in Switzerland the following week. The longest core retrieved (425 cm) was subsampled at 1 cm resolution following XRF scanning and samples were then freeze-dried. Macrofossils were separated for radiocarbon measurements. The sub-sample was then split with 1.5 cm^3 used for bulk analyses while the rest of the sediment was used for biomarker extraction (up to ~3 g of dried sediment).

Chronology

Radiocarbon dating of 57 macrofossils from 48 unique depths (supplementary table S1) was carried out at the Laboratory of Ion Beam Physics of ETH Zurich. Plant remains (wood, seeds and leaves) were chosen for the measurements. After an acid-base-acid chemical cleaning treatment[88] 41 samples underwent graphitization before measurement, while smaller samples were directly measured with an accelerator mass spectrometer[89]. Data evaluation and corrections were done following the procedures described in Welte et al.[90]. R Statistical Software (v4.2.0, R core team 2022) was used to perform all data analysis and visualisation. The age-depth deposition model was performed with the package rbacon version 2.5.8[91]. Radiocarbon dates were calibrated with the Southern Hemisphere calibration curve shcal13[92]. Seventeen samples were excluded from the model. Of these, seven samples were identified as root intrusions, and eight samples were excluded as their older ages and δ13C values above -15‰ indicate that these samples integrated old carbon derived from the limestone catchment. Postbomb dates were not included in the age depth model.

Bulk geochemical analyses

Bulk geochemical analyses were carried out in the Sedimentology laboratories at Eawag, Dübendorf. Downcore total carbon (TC) and total nitrogen (TN) content were measured with an EURO Elemental Analyser (EA) 3000 for a total of 104 samples. Total inorganic carbon (TIC) was measured with a titration Coulometer (CM5015). Total organic carbon (TOC) was calculated using the equation TOC = TC – TIC. The bulk sediment $\delta^{15}N$ was measured on an EA-IRMS (EA Vario Pyro Cube by Elementar and IRMS by GV Instruments, Isoprime). Elemental counts were measured using an Avaatech XRF core scanner with an Oxford 100

Watt X-ray source with Rhodium anode and Canberra X – Pips and Canberra DSA 1000 (MCA) detector. The sediment and peat core sections were carefully levelled and covered with a 4 μm thick ultralene plastic film. Two different settings were applied for the scan: 10 kV with 30 seconds count time, no filter for the lighter elements, and 30 kV with thin Pd filter and 30 seconds count time for the heavier elements. Step size was 5 mm.

Biomarker analysis

Lipid extraction, purification and quantification were performed in the Sedimentology laboratories at Eawag, Dübendorf. Total lipid content was extracted from 112 sediment samples distributed along the core length. Sediment samples were extracted in a mixture of DCM/MeOH (9:1, v/v) with a Dionex ASE 350 (Thermo Scientific). Lipid saponification and column chromatography of the neutral fraction and derivatization of the sterols were performed as in Krentscher et al.[45]. The acid fraction was separated, methylated and purified as in Ladd et al.[47].

Compounds were identified and quantified by gas chromatography–mass spectrometry (GC–MS) as described in Krentscher et al.[45]. Ketones and the derivatized sterols were run with a Selected Ion Monitoring method targeting ions (Supplementary Information). An external standard with the targeted compounds was added for identification and quantification via external calibration curve. The ratio between the sum of coprostanol and epicoprostanol and cholestanol was included in the results (see Supplementary Figure 6 for details).

The hydrogen isotopic analyses of leaf waxes were performed in the Stable Isotope Ecology Lab at the University of Basel. The samples were analysed on a Trace GC Ultra gas chromatograph (GC) coupled to a Thermo Delta V Plus isotope ratio mass spectrometer (IRMS) via a GC Isolink operated in pyrolysis mode and ConFlo IV interface (Thermo Fisher Scientific, Bremen, Germany). The measured values were normalised to the VSMOW/SLAP scale using hydrogen isotope standards purchased from Arndt Schimmelmann at Indiana University. Measurement accuracy and precision were assessed from a quality control standard, a hydrocarbon fraction from oak leaves that were originally collected in Berkeley, California. The average δ^2H value of the n-C29 alkane in this standard is -142.4 ± 3.7 ‰ (n = 868, going back to 2014). The standard was analysed 53 times with our sample set, with a mean δ^2H value of -141.4‰ , which is offset from the calibrated value by 1.2 ‰. The standard deviation of these analyses was 1.6 ‰. Additional details on the robustness of the δ^2H signal can be found in the Supplementary Information and Supplementary Figures S7 - S10.

Acknowledgments

The research permit was approved by the Vanuatu National Cultural Council and the Department of Environmental Protection and Conservation (DEPC). We thank Richard Shing and Henline Mala from the Vanuatu Cultural Center and Reedly Tari, Donna Kalfatakmoli and Primrose Malosu from DEPC for their guidance in the permit process. Danny Nef assisted with 2017 field work. Irene Brunner from the sedimentology group at Eawag conducted bulk analysis, Caroline Welte, Silvia Bollhalder, and Karin Wyss Heeb from the Ion Beam Physics department of ETH Zurich, and Anita Schlatter from the sedimentology group, Eawag, helped with the radiocarbon dating. We thank the Teouma site leaseholder M. Robert Monvoisin for granting permission to access and core in their land and Stuart Bedford for support in the field as well as for constructive feedback. We thank Charmaine Bassfeld, Shannon Dyer, Erik Hegenberg, Gioele Scacco, and Lucas Soliva for technical support. We thank Gabriele Consoli, Irka Hajdas, Dave Jansen, Benjamin Keenan, Nannan Li, and Tobias Schneider for their constructive feedback during the preparation of this manuscript.

Author contributions

ND and MP conceived the project. ND acquired the funding for the project. SNL and GC contributed to the design of the study. ND and GC coordinated the study. ND, MP, SNL, RL, and GC conducted the fieldwork. CK, EA, SNL, RL, ND and GC conducted the lipid biomarker quantification and interpretation. DBN and SNL performed the compound specific stable isotope analyses. RL and GC performed the XRF core scanning and grain size analysis. ND directed the bulk geochemical analyses. GC created the figures and led the writing of the paper to which all authors contributed. All authors discussed the results and commented on the manuscript.

Competing interest

The authors declare that they have no competing interests.

Funding

This work is part of the Swiss National Science Foundation (SNSF) funded MACRO project (Grant Nr. PP00P2_163782 to ND). Additional laboratory work was funded by the Tailwind grant of Eawag Switzerland to GC.

Supplementary Information is available for this paper.

Materials & Correspondence

Correspondence and material requests should be addressed to the corresponding author Giorgia Camperio

Data availability

Data will be made available on the PANGEA repository at the time of publication.

Figures and figure captions

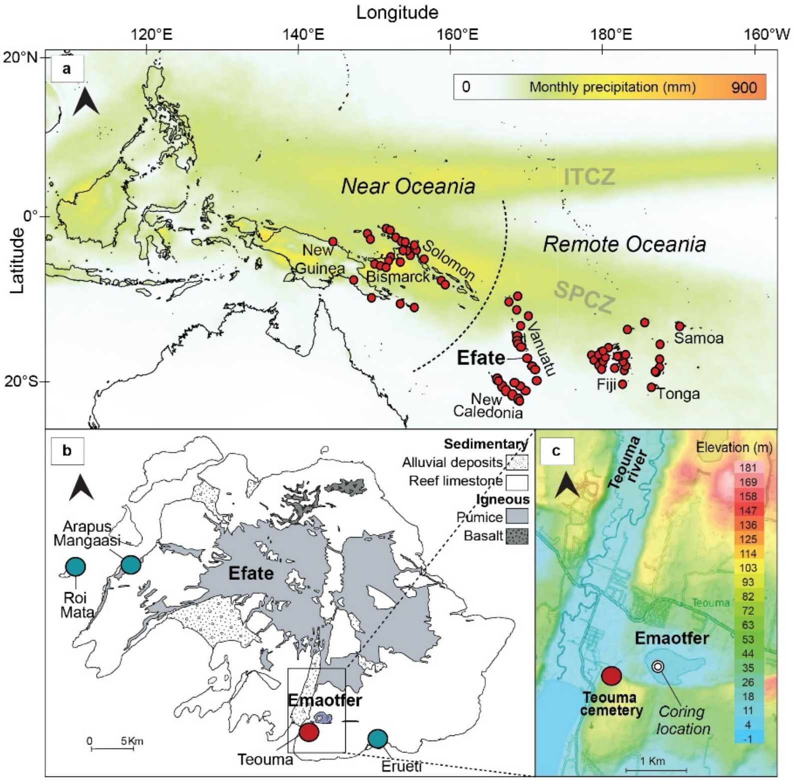

Figure 1. Map of Emaotfer swamp on the island of Efate, Vanuatu in relation to the Lapita archaeological sites across remote Oceania (A) Map of the Lapita archaeological sites (red dots) on tropical Pacific islands. Curved dashed line delimits Near Oceania and Remote Oceania[93]. Shading corresponds to monthly precipitation[94] (source of data https://disc.gsfc.nasa.gov/datasets/GPM_3IMERGM_06/summary). (B) Geological map of Efate (Vanuatu). Dots correspond to the archaeological sites discussed in the text, blue shading indicates the location of Emaotfer Swamp. (C) Elevation map of the Teouma area with the Teouma archaeological site (red dot) and the Teouma river to the west of Emaotfer swamp, coring location shown in the swamp (map from https://en-gb.topographic-map.com/).

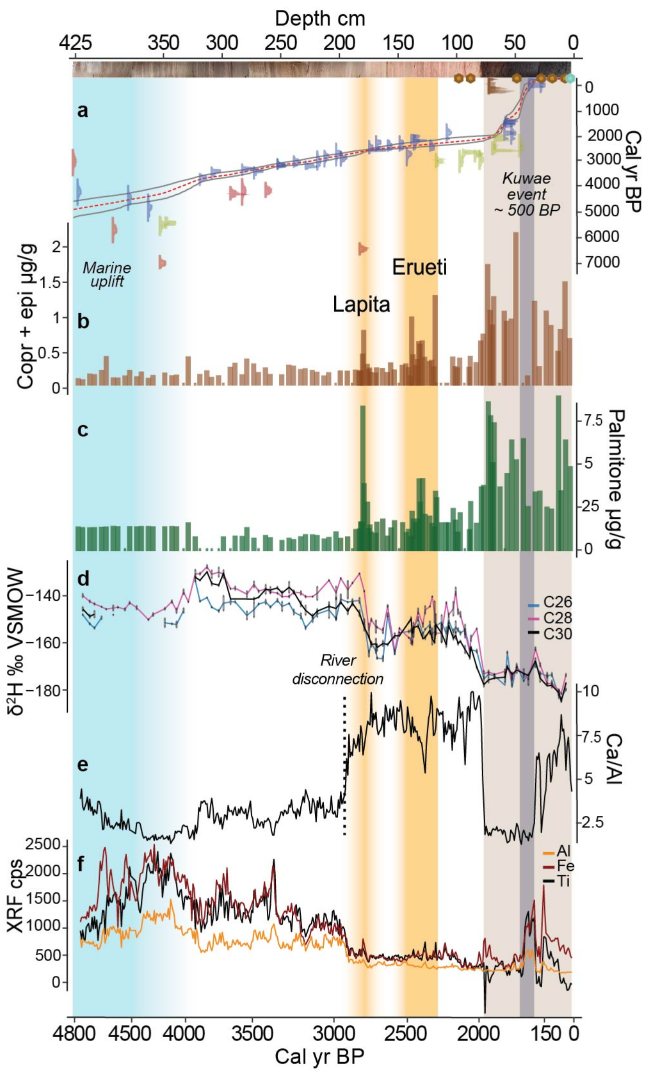

Figure 2. Downcore fossil biomarker record of Efate tracking human presence, horticulture and paleoclimatic shifts along the paleoenvironmental record from XRF elemental counts. (A) Age-depth model using the r package rbacon version 3.0.0[91]. Green hexagon for coring year (2017), brown hexagons for postbomb roots, brown age calibration pre-bomb roots. Yellow age calibration for samples that incorporated old carbon (δ13C above -15‰). Blue plots represent the age distribution of macrofossils used in the age model red for those that were excluded from the model. Grey lines indicate respectively the minimum and maximum range of calibrated ages. Red line indicates the median calibrated ages. (B) Coprostanol and epicoprostanol concentrations are indicated with brown bars, (C) palmitone with green bars both in µg/g of sediment. (D) Compound specific n-alkanoic acids δ^2H in black

(C30), in light pink (C28), and light blue (C26), in permil V-SMOW. (E+F) Changes in the elemental composition of the core measured with an XRF core scanner, with (E) the calcium to aluminum ratio (Ca/Al) in black and (F) terrigenous elements in black (titanium), red (iron), and orange (aluminium) in counts per seconds (cps). Light blue shading represents the marine period of the basin, yellow shadings represent periods of human occupation corresponding to the Lapita and Erueti phase in the archaeological record, brown shading indicates the peat part of the core, grey area indicates the possible location of the Kuwae volcanic tephra (1452 or 1453 CE[95]).

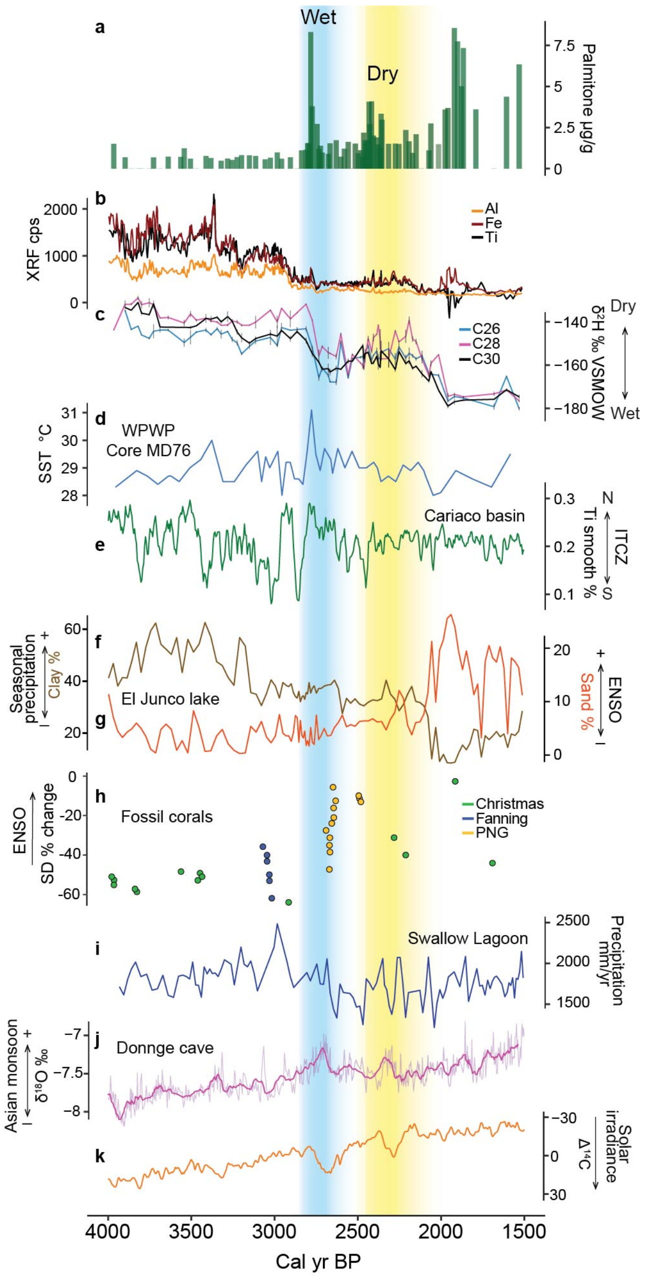

Figure 3. Climatic reconstructions for the period 4000 - 1500 BP across the Pacific. (A) Palmitone concentrations (green bars). (B) XRF counts per second of terrigenous elements, black (titanium), red (iron), and orange (aluminium). (C) Compound specific n-alkanoic acids δ^2H in black (C30), blue (C28), and light pink (C26), in permil V-SMOW. (D) WPWP sea surface temperature reconstruction for core MD76 (lightblue) (Stott et al., 2004). (E) Titanium % from the Cariaco Basin in green[71]. (F+G) Grain Size from El Junco lake, Galapagos, with (F) clay (brown) and (G) sand (yellow)[73]. (H) Calculations of standard deviation of 2 to 7 year band of fossil coral $\delta^{18}O$ time series calculated as percentage difference from modern coral reference following Cobb et al.[76], Christmas Island[76,96] and its micro-atolls[97] in green, Fanning island in blue[76] (Cobb et al. 2013), and Papua New Guinea in gold[78,98]. (I) Mean annual precipitation from Swallow Lagoon[77]. (J) $\delta^{18}O$ from the Donnge Cave (pink)[72]. (K) Southern hemisphere solar radiative force (orange)[92]. Colour shading indicates wet (light blue) and dry (yellow) hydroclimatic phases.

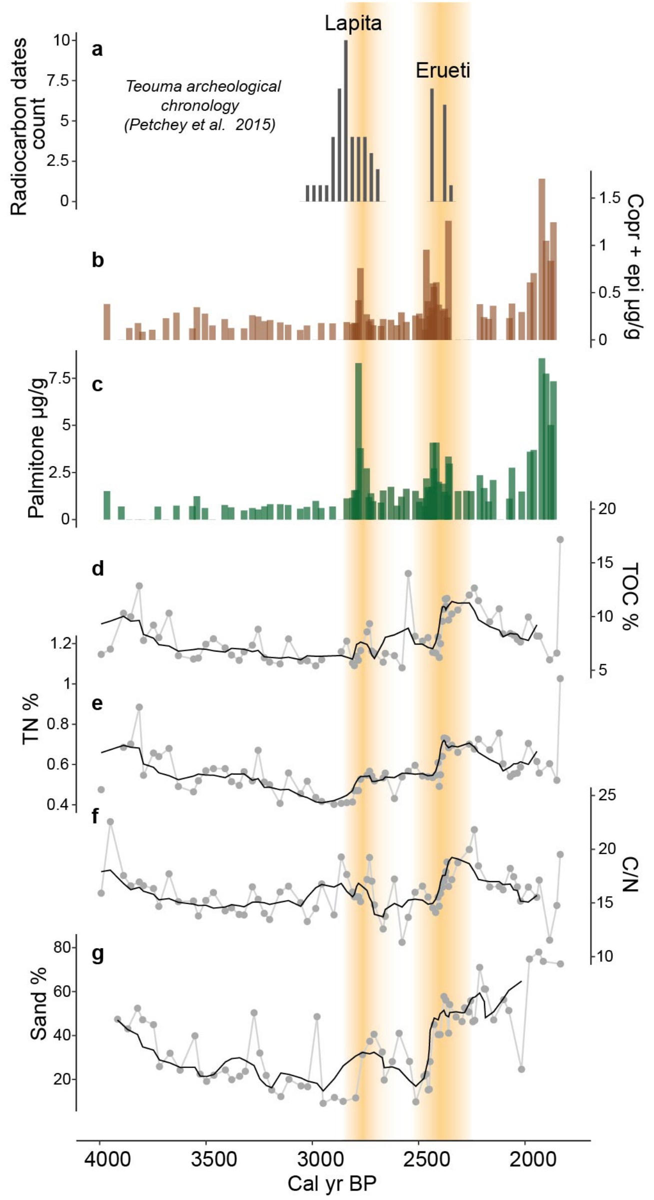

Figure 4. Environmental changes during the Lapita and Erueti settlement. (A): Histogram of median calibrated ages for the Lapita period combined with age range of the Erueti period unmodeled calibrated ages (68% prob)[22]. (B) Sum of coprostanol and epicoprostanol showing faecal markers concentrations as brown bars. (C) Palmitone concentrations as green bars. Black lines indicate five-point averages for (D) total organic carbon (TOC), (E) total nitrogen (TN), (F) C/N ratio, and (G) sand fraction. Yellow shades indicate periods of human occupation.

References

1. Hunt, T. L. & Lipo, C. P. The last great migration: Human colonization of the Remote Pacific Islands. in *Human Dispersal and Species Movement* (eds. Boivin, N., Crassard, R. & Petraglia, M.) 194–216 (Cambridge University Press, 2017).

2. Skoglund, P. et al. Genomic insights into the peopling of the Southwest Pacific. *Nature* **538**, 510–513 (2016).

3. Lipson, M. et al. Population Turnover in Remote Oceania Shortly after Initial Settlement. *Curr. Biol.* **28**, 1157-1165.e7 (2018).

4. Pugach, I. et al. The Gateway from Near into Remote Oceania: New Insights from Genome-Wide Data. *Mol. Biol. and Evol.* **35**, 871–886 (2018).

5. Choin, J. et al. Genomic insights into population history and biological adaptation in Oceania. *Nature* **592**, 583–589 (2021).

6. Shaw, B. et al. Frontier Lapita interaction with resident Papuan populations set the stage for initial peopling of the Pacific. *Nat. Ecol. Evol.* **6**, 802–812 (2022).

7. Hermann, A. et al. Artifact geochemistry demonstrates long-distance voyaging in the Polynesian Outliers. *Sci.Adv*. **9**, eadf4487 (2023).

8. Kirch, P. V. *On the road of the winds: an archaeological history of the Pacific Islands before European contact*. (Univ of California Press, 2017).

9. Spriggs, M. *The Island Melanesians*. (Oxford: Blackwell, 1997).

10. Spriggs, M. The Lapita Culture and Austronesian Prehistory in Oceania. in *The Austronesians* (eds. Bellwood, P., Fox, J. J. & Tryon, D.) 119–142 (ANU Press, 2006).

11. Anderson, A., Chappell, J., Gagan, M. & Grove, R. Prehistoric maritime migration in the Pacific islands: an hypothesis of ENSO forcing. *The Holocene* **16**, 1–6 (2006).

12. Goodwin, I. D., Browning, S. A. & Anderson, A. J. Climate windows for Polynesian voyaging to New Zealand and Easter Island. *Proc. Natl. Acad. Sci. U.S.A.* **111**, 14716–14721 (2014).

13. Montenegro, Á., Callaghan, R. T. & Fitzpatrick, S. M. Using seafaring simulations and shortest-hop trajectories to model the prehistoric colonization of Remote Oceania. *Proc. Natl. Acad. Sci. U.S.A.* **113**, 12685–12690 (2016).

14. Clark, G. & Reepmeyer, C. Last millennium climate change in the occupation and abandonment of Palau's Rock Islands. *Archaeol. Ocean.* **47**, 29–38 (2012).

15. Sear, D. A. et al. Human settlement of East Polynesia earlier, incremental, and coincident with prolonged South Pacific drought. *Proc. Natl. Acad. Sci. U.S.A.* **117**, 8813–8819 (2020).

16. Bonsall, C., Macklin, M. G., Anderson, D. E. & Payton, R. W. Climate change and the adoption of agriculture in north-west Europe. *Eur. J. Archaeol.* **5**, 9–23 (2002).

17. Piperno, D. R. The Origins of Plant Cultivation and Domestication in the New World Tropics: Patterns, Process, and New Developments. *Curr. Anthropol.* **52**, S453–S470 (2011).

18. Duncan, N. A., Loughlin, N. J. D., Walker, J. H., Hocking, E. P. & Whitney, B. S. Pre-Columbian fire management and control of climate-driven floodwaters over 3,500 years in southwestern Amazonia. *Proc. Natl. Acad. Sci. U.S.A.* **118**, e2022206118 (2021).

19. Shaw, B. et al. 2500-year cultural sequence in the Massim region of eastern Papua New Guinea reflects adaptive strategies to small islands and changing climate regimes since Lapita settlement. *The Holocene* **30**, 1075–1090 (2020).

20. Bedford, S. & Spriggs, M. The Archaeology of Vanuatu: 3000 Years of History across Islands of Ash and Coral. in *The Oxford Handbook of Prehistoric Oceania (*eds. Ethan E. Cochrane, E.E. & Hunt, T. L.) 162–184 (Oxford Academic 2014).

21. Bedford, S., Hoffman, A., Kaltal, M., Regenvanu, R. & Shing, R. Dentate-stamped Lapita reappears on Efate, Central Vanuatu: A four decade-long drought is broken. *Archaeology in New Zealand* **47**, 39–49 (2004).

22. Petchey, F., Spriggs, M., Bedford, S. & Valentin, F. The chronology of occupation at Teouma, Vanuatu: Use of a modified chronometric hygiene protocol and Bayesian modeling to evaluate midden remains. *Journal of J. Archaeol. Sci. Rep.* **4**, 95–105 (2015).

23. Burley, D., Weisler, M. I. & Zhao, J. High Precision U/Th Dating of First Polynesian Settlement. *PLoS ONE* **7**, e48769 (2012).

24. Petchey, F., Spriggs, M., Bedford, S., Valentin, F. & Buckley, H. Radiocarbon dating of burials from the Teouma Lapita cemetery, Efate, Vanuatu. *J. Archaeol. Sci.* **50**, 227–242 (2014).

25. Spriggs, M. J. T. *Vegetable kingdoms : taro irrigation and Pacific prehistory*. (The Australian National University 1981)

26. Horrocks, M. & Bedford, S. Microfossil Analysis of Lapita Deposits in Vanuatu Reveals Introduced Araceae (Aroids). *Archaeol. Oceania* **40**, 67–74 (2005).

27. Horrocks, M. & Bedford, S. Introduced Dioscorea spp. starch in Lapita and later deposits, Vao Island, Vanuatu. *N. Z. J. Bot.* **48**, 179–183 (2010).

28. Tromp, M. et al. Exploitation and utilization of tropical rainforests indicated in dental calculus of ancient Oceanic Lapita culture colonists. *Nat. Hum. Behav.* **4**, 489–495 (2020).

29. Lentfer, C. J., Crowther, A. & Green, R. C. The question of Early Lapita settlements in Remote Oceania and reliance on horticulture revisited: new evidence from plant microfossil studies at Reef/Santa Cruz, south-east Solomon Islands. *Technical Reports of the Australian Museum* **34**, 87–106 (2021).

30. Simeoni, P. *Atlas du Vanouatou (Vanuatu).* (Port-Vila: Géo-consulte 2009).

31. Vincent, D. G. The South Pacific Convergence Zone (SPCZ): A Review. *Mon. Weather Rev.* **122**, 1949–1970 (1994).

32. Brown, J. R. et al. South Pacific Convergence Zone dynamics, variability and impacts in a changing climate. *Nat. Rev. Earth. Environ*. **1**, 530–543 (2020).

33. Folland, C. K. Relative influences of the Interdecadal Pacific Oscillation and ENSO on the South Pacific Convergence Zone. *Geophys. Res. Lett.* **29**, 1643 (2002).

34. Saint-Lu, M., Braconnot, P., Leloup, J., Lengaigne, M. & Marti, O. Changes in the ENSO/SPCZ relationship from past to future climates. *Earth Planet. Sci. Lett*. **412**, 18–24 (2015).

35. McNamara, K. E. & Prasad, S. S. Coping with extreme weather: communities in Fiji and Vanuatu share their experiences and knowledge. *Clim. Change* **123**, 121–132 (2014).

36. Bedford, S., Spriggs, M. & Regenvanu, R. The Teouma Lapita site and the early human settlement of the Pacific Islands. *Antiquity* **80**, 812–828 (2006).

37. Bedford, S. et al. A cemetery of first settlement: The site of Teouma, South Efate, Vanuatu. *Lapita: Oceanic Ancestors,* 140–161 (2010).

38. Bethell, P. H., Goad, L. J., Evershed, R. P. & Ottaway, J. The Study of Molecular Markers of Human Activity: The Use of Coprostanol in the Soil as an Indicator of Human Faecal Material. *J. Archaeol. Sci.* **21**, 619–632 (1994).

39. White, A. J. et al. Fecal stanols show simultaneous flooding and seasonal precipitation change correlate with Cahokia's population decline. *Proc. Natl. Acad. Sci. U.S.A.* **116**, 5461–5466 (2019).

40. Keenan, B. et al. Molecular evidence for human population change associated with climate events in the Maya lowlands. *Quat. Sci. Rev.* **258**, 106904 (2021).

41. Pawley, A. Were the First Lapita Colonisers of Remote Oceania Farmers as Well as Foragers? in *New perspectives in Southeast Asian and Pacific prehistory* (ed. Piper P. J.) 293–310 (ANU Press 2017).

42. Horrocks, M. & Nunn, P. D. Evidence for introduced taro (Colocasia esculenta) and lesser yam (Dioscorea esculenta) in Lapita-era (c. 3050–2500cal.yrBP) deposits from Bourewa, southwest Viti Levu Island, Fiji. *J. Archaeol. Sci.* **34**, 739–748 (2007).

43. Prebble, M. & Wilmshurst, J. M. Detecting the initial impact of humans and introduced species on island environments in Remote Oceania using palaeoecology. *Biol. Invasions* **11**, 1529–1556 (2009).

44. Prebble, M. et al. Early tropical crop production in marginal subtropical and temperate Polynesia. *Proc. Natl. Acad. Sci. U.S.A.* **116**, 8824–8833 (2019).

45. Krentscher, C., Dubois, N., Camperio, G., Prebble, M. & Ladd, S. N. Palmitone as a potential species-specific biomarker for the crop plant taro (Colocasia esculenta Schott) on remote Pacific islands. *Org. Geochem.* **132**, 1–10 (2019).

46. Sachse, D. et al. Molecular Paleohydrology: Interpreting the Hydrogen-Isotopic Composition of Lipid Biomarkers from Photosynthesizing Organisms. *Annu. Rev. Earth Planet. Sci.* **40**, 221–249 (2012).

47. Ladd, S. N. et al. Leaf Wax Hydrogen Isotopes as a Hydroclimate Proxy in the Tropical Pacific. Journal of Geophysical Research: *Biogeosciences* **126**, e2020JG005891 (2021).

48. Robin, C., Australian Geological Survey Organisation, & IAVCEI General Assembly. *The Geology, volcanology, petrology-geochemistry, and tectonic evolution of the New Hebrides Island Arc, Vanuatu: IAVCEI, Canberra 1993 : excursion guide.* (Australian Geological Survey Organisation, 1993).

49. Bedford, S., Spriggs, M., Buckley, H. R., Valentin, F., & Regenvanu, R. The Teouma Lapita site, South Efate, Vanuatu: a summary of three field seasons (2004-2006). in *Lapita: Ancestors and Descendant* (ed. Sheppard P., Thomas T., Summerhayes G.) 215–234 (NewZealand Archaeological Association, Auckland, 2009).

50. Dickinson, W. R. Paleoshoreline record of relative Holocene sea levels on Pacific islands. *Earth-Sci. Rev.* **55**, 191–234 (2001).

51. Combettes, C., Sémah, A.-M. & Wirrmann, D. High-resolution pollen record from Efate Island, central Vanuatu: Highlighting climatic and human influences on Late Holocene vegetation dynamics. *C. R. –Palevol.* **14**, 251–261 (2015).

52. Bedford, S., Siméoni, P. & Lebot, V. The anthropogenic transformation of an island landscape: Evidence for agricultural development revealed by LiDAR on the island of Efate, Central Vanuatu, South-West Pacific. *Archaeol. Ocean.* **53**, 1–14 (2018).

53. Spriggs, M. Taro Cropping Systems in the Southeast Asian-Pacific Region: Archaeological Evidence. *Archaeol. Ocean* **17**, 7–15 (1982).

54. Weightman, B. *Agriculture in Vanuatu: a historical review*. (The British Friends of Vanuatu 1989).

55. Burley, D. V., Horrocks, M. & Weisler, M. I. Earliest Evidence for Pit Cultivation Provides Insight on the Nature of First Polynesian Settlement. *J. Isl. Coast. Archaeol.* **15**, 127–147 (2020).

56. Dubois, N. et al. First human impacts and responses of aquatic systems: A review of palaeolimnological records from around the world. *Anthr. Rev.* **5**, 28–68 (2018).

57. Rothwell, R. G. & Croudace, I. w. Twenty Years of XRF Core Scanning Marine Sediments: What Do Geochemical Proxies Tell Us? in *Micro-XRF Studies of Sediment Cores: Applications of a non-destructive tool for the environmental sciences* (eds. Croudace, I. W. & Rothwell, R. G.) 25–102 (Springer Netherlands, 2015).

58. Kinaston, R. et al. Lapita Diet in Remote Oceania: New Stable Isotope Evidence from the 3000-Year-Old Teouma Site, Efate Island, Vanuatu. *PLoS ONE* **9**, e90376 (2014).

59. Valentin, F. et al. Lapita subsistence strategies and food consumption patterns in the community of Teouma (Efate, Vanuatu). *J. Archaeol. Sci.* **37**, 1820–1829 (2010).

60. Anderson, A. The rat and the octopus: initial human colonization and the prehistoric introduction of domestic animals to Remote Oceania. *Biol. Invasions* **11**, 1503–1519 (2009).

61. Valentin, F., Détroit, F., Spriggs, M. J. T. & Bedford, S. Early Lapita skeletons from Vanuatu show Polynesian craniofacial shape: Implications for Remote Oceanic settlement and Lapita origins. *Proc. Natl. Acad. Sci. U.S.A.* **113**, 292–297 (2016).

62. Posth, C. et al. Language continuity despite population replacement in Remote Oceania. *Nat. Ecol. Evol.* **2**, 731–740 (2018).

63. Dickinson, W. R. & Green, R. C. Geoarchaeological context of Holocene subsidence at the Ferry Berth Lapita site, Mulifanua, Upolu, Samoa. *Geoarchaeology* **13**, 239–263 (1998).

64. Bedford, S. *Pieces of the Vanuatu Puzzle: Archaeology of the North, South and Centre*. (ANU press 2006).

65. Garanger, J. Arch eologie des Nouvelles H ebrides: Contribution a la connaissance des ıles du Centre. *Publications de la Société des Océanistes* **30**, (1972).

66. Atwood, A. R., Battisti, D. S., Wu, E., Frierson, D. M. W. & Sachs, J. P. Data-Model Comparisons of Tropical Hydroclimate Changes Over the Common Era. *Paleoceanogr. Paleoclimatol*. **36**, e2020PA003934 (2021).

67. Hassall, J. D. *Static or dynamic: Reconstructing past movement of the South Pacific Convergence Zone*. (University of Southampton 2017).

68. Stott, L. et al. Decline of surface temperature and salinity in the western tropical Pacific Ocean in the Holocene epoch. *Nature* **431**, 56–59 (2004).

69. van der Wiel, K., Matthews, A. J., Joshi, M. M. & Stevens, D. P. Why the South Pacific Convergence Zone is diagonal. *Clim. Dyn.* **46**, 1683–1698 (2016).

70. Mantsis, D. F., Lintner, B. R., Broccoli, A. J. & Khodri, M. Mechanisms of Mid-Holocene Precipitation Change in the South Pacific Convergence Zone. *J. Clim.* **26**, 6937–6953 (2013).

71. Haug, G. H., Hughen, K. A., Sigman, D. M., Peterson, L. C. & Röhl, U. Southward Migration of the Intertropical Convergence Zone Through the Holocene. *Science* **293**, 1304–1308 (2001).

72. Wang, Y. et al. The Holocene Asian Monsoon: Links to Solar Changes and North Atlantic Climate. *Science* **308**, 854–857 (2005).

73. Conroy, J. L., Overpeck, J. T., Cole, J. E., Shanahan, T. M. & Steinitz-Kannan, M. Holocene changes in eastern tropical Pacific climate inferred from a Galápagos lake sediment record. *Quat. Sci. Rev.* **27**, 1166–1180 (2008).

74. Karamperidou, C. & DiNezio, P. N. Holocene hydroclimatic variability in the tropical Pacific explained by changing ENSO diversity. *Nat. Commun.* **13**, 7244 (2022).

75. Murphy, B. F., Power, S. B. & McGree, S. The Varied Impacts of El Niño–Southern Oscillation on Pacific Island Climates. *J. Clim.* **27**, 4015–4036 (2014).

76. Cobb, K. M. et al. Highly Variable El Niño–Southern Oscillation Throughout the Holocene. *Science* **339**, 67–70 (2013).

77. Barr, C. et al. Holocene El Niño–Southern Oscillation variability reflected in subtropical Australian precipitation. *Sci. Rep.* **9**, 1627 (2019).

78. McGregor, H. V. & Gagan, M. K. Western Pacific coral δ18O records of anomalous Holocene variability in the El Niño–Southern Oscillation. *Geophys. Res. Lett.* **31**, (2004).

79. Nelson, D. B. & Sachs, J. P. Galápagos hydroclimate of the Common Era from paired microalgal and mangrove biomarker 2 H/ 1 H values. *Proc. Natl. Acad. Sci. U.S.A*. **113**, 3476–3481 (2016).

80. Wirrmann, D., Eagar, S. H., Harper, M. A., Leroy, É. & Sémah, A.-M. First insights into mid-Holocene environmental change in central Vanuatu inferred from a terrestrial record from Emaotfer Swamp, Efaté Island. *Quat. Sci. Rev* **30**, 3908–3924 (2011).

81. Bostoen, K. et al. Middle to Late Holocene Paleoclimatic Change and the Early Bantu Expansion in the Rain Forests of Western Central Africa. *Curr. Anthropol.* **56**, 354–384 (2015).

82. Bunbury, M. M. E., Petchey, F. & Bickler, S. H. A new chronology for the Māori settlement of Aotearoa (NZ) and the potential role of climate change in demographic developments. *Proc. Natl. Acad. Sci. U.S.A*. **119**, e2207609119 (2022).

83. D'Andrea, W. J., Huang, Y., Fritz, S. C. & Anderson, N. J. Abrupt Holocene climate change as an important factor for human migration in West Greenland. *Proc. Natl. Acad. Sci. U.S.A*. **108**, 9765–9769 (2011).

84. Friesen, T. M., Finkelstein, S. A. & Medeiros, A. S. Climate variability of the Common Era (AD 1–2000) in the eastern North American Arctic: Impacts on human migrations. *Quat. Int.* **549**, 142–154 (2020).

85. Raposeiro, P. M. et al. Climate change facilitated the early colonization of the Azores Archipelago during medieval times. *Proc. Natl. Acad. Sci. U.S.A.* **118**, e2108236118 (2021).

86. Zhao, B. et al. Prolonged drying trend coincident with the demise of Norse settlement in southern Greenland. *Sci. Adv.* **8**, eabm4346 (2022).

87. Valentin, F., Herrscher, E., Bedford, S., Spriggs, M. & Buckley, H. Evidence for Social and Cultural Change in Central Vanuatu Between 3000 and 2000 BP: Comparing Funerary

and Dietary Patterns of the First and Later Generations at Teouma, Efate. *J. Isl. Coast. Archaeol*. **9**, 381–399 (2014).

88. Hajdas, I. et al. AMS radiocarbon dating of annually laminated sediments from lake Holzmaar, Germany. *Quat. Sci. Rev.* **14**, 137–143 (1995).

89. Wacker, L. et al. MICADAS: Routine and High-Precision Radiocarbon Dating. *Radiocarbon* **52**, 252–262 (2010).

90. Welte, C. et al. Towards the limits: Analysis of microscale 14C samples using EA-AMS. *Nucl. Instrum. Methods Phys. Res.* **437**, 66–74 (2018).

91. Blaauw, M. & Christen, J. A. Flexible paleoclimate age-depth models using an autoregressive gamma process. *Bayesian Anal.* **6**, 457–474 (2011).

92. Hogg, A. G. et al. SHCal20 Southern Hemisphere Calibration, 0–55,000 Years cal BP. *Radiocarbon* **62**, 759–778 (2020).

93. Green, R. Near and Remote Oceania: disestablishing" Melanesia" in culture history. in *Man and a half: Essays in Pacific Anthropology and Ethnobotany in honour of Ralph Bulmer* (ed. Pawley, A.) 91-502 (The Polynesian Society 1991).

94. Huffman, G.J. et al. GPM IMERG Final Precipitation L3 1 month 0.1 degree x 0.1 degree V06, Greenbelt, MD, Goddard Earth Sciences Data and Information Services Center (GES DISC) (2019). 10.5067/GPM/IMERGDF/DAY/06

95. Gao, C. et al. The 1452 or 1453 A.D. Kuwae eruption signal derived from multiple ice core records: Greatest volcanic sulfate event of the past 700 years. *J. Geophys. Res.* **111**, D12107 (2006).

96. Zaunbrecher, L. K. et al. Coral records of central tropical Pacific radiocarbon variability during the last millennium. *Paleoceanogr.* **25**, (2010).

97. Woodroffe, C. D., Beech, M. R. & Gagan, M. K. Mid-late Holocene El Niño variability in the equatorial Pacific from coral microatolls. *Geophys. Res. Lett.* **30**, (2003).

98. Tudhope, A. W. et al. Variability in the El Niño-Southern Oscillation Through a Glacial-Interglacial Cycle. *Science* **291**, 1511–1517 (2001).

Supplementary information for

Wetter climate favouring early Lapita horticulture in Remote Oceania

Giorgia Camperio[1,2*], S. Nemiah Ladd[3], Matiu Prebble[4,5], Ronald Lloren[1,2], Elena Argiriadis[6,7], Daniel B. Nelson[8], Christiane Krentscher[1], Nathalie Dubois[1,2]

*Corresponding author: giorgia.camperio@eawag.ch

Affiliations

[1]Department of Surface Waters Research & Management, Eawag, Dübendorf, 8600, Switzerland

[2]Department of Earth Sciences, ETH Zürich, Zürich, 8092, Switzerland

[3]Department of Environmental Sciences, University of Basel, Basel, 4056, Switzerland

[4]School of Earth and Environment, College of Science, University of Canterbury, Christchurch, 8041, New Zealand

[5]Archaeology and Natural History, Culture History and Languages, The Australian National University, Canberra, ACT 2010, Australia

[6]Institute of Polar Sciences, CNR-ISP, Venice, 30172, Italy

[7]Department of Environmental Sciences, Informatics and Statistics, Ca' Foscari University, Venice, 30172, Italy

[8]Department of Environmental Sciences – Botany, University of Basel, 4056, Basel, Switzerland

This PDF file includes:

Figures S1 to S10

Table S1, S2

Supporting text

SI References

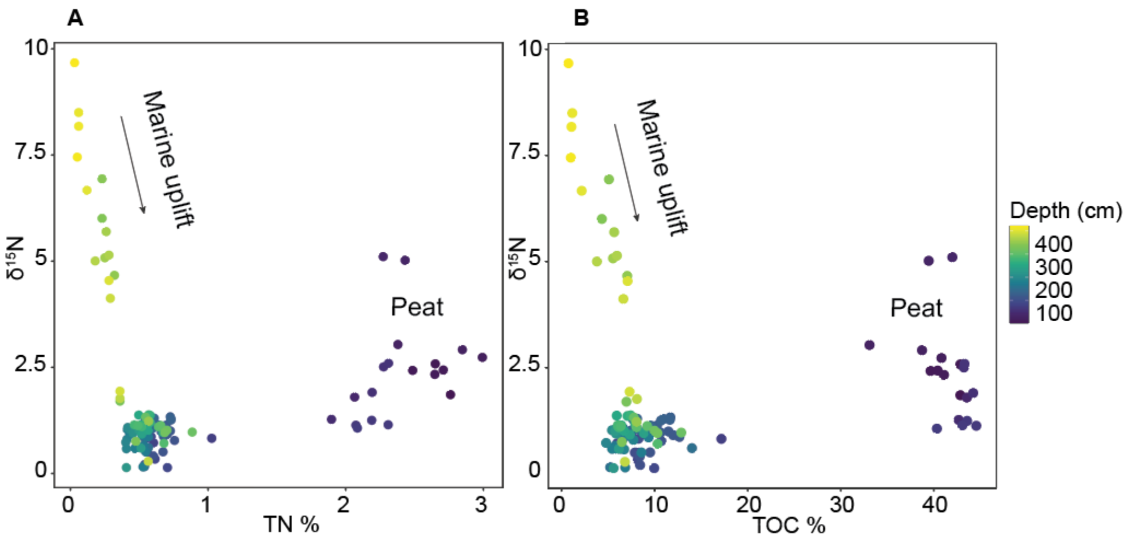

Supplementary figure S1. **Bulk sediment geochemistry of the Emaotfer sediment core showing its three main depositional phases.** A) Crossplot of C/N ratios against δ13C of bulk sediment, B) crossplot of δ15N and δ13C. Colour indicates the depth of samples. Yellowish colour corresponds to the marine phase, green to the lacustrine phase, and blue to the peat.

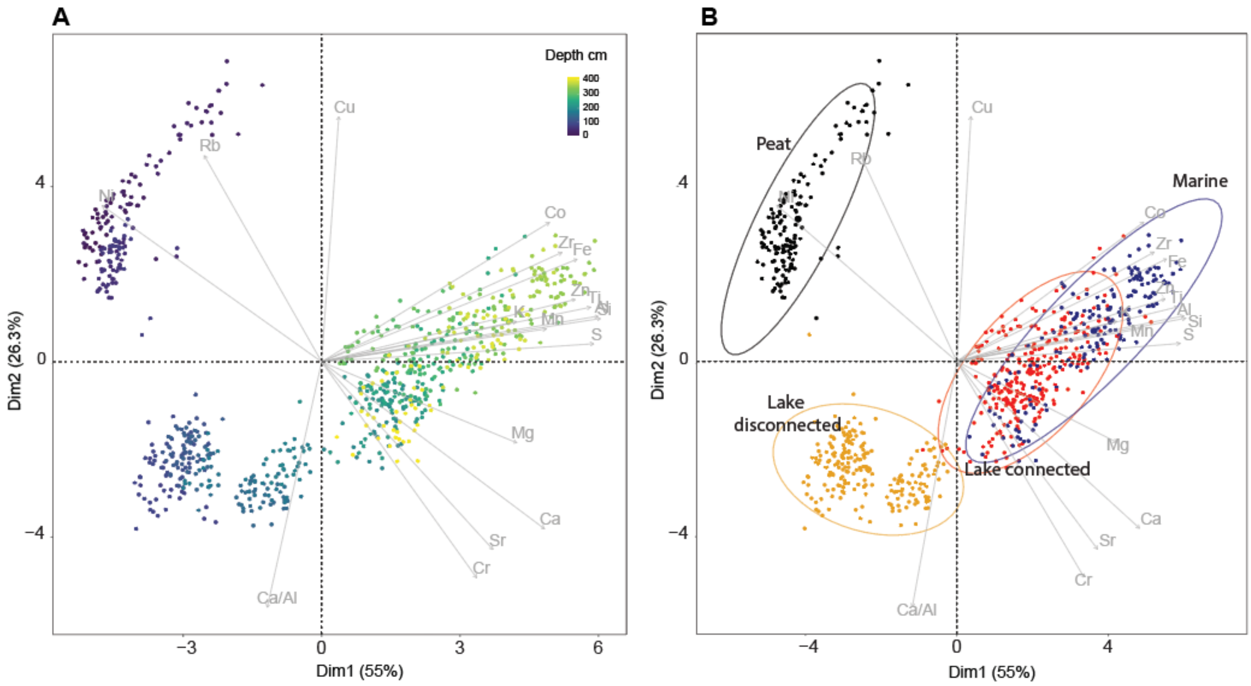

Supplementary figure S2. **Principal component analysis of the downcore XRF elemental distribution.** Arrows indicate the contribution of each element. (A) Colour indicates the depth of samples. (B) Depositional phases are circled: peat (black), lake disconnected from the Teouma river (orange), lake connected (red), and marine (dark blue) phase (high terrestrial elements).

Supplementary Information SI1 XRF elemental data

In these settings, Al, Fe, and Ti reflect terrigenous input[1] delivered by the nearby Teouma river, which transports elements collected along its catchment (see pumice and alluvial deposits on Figure 1). Calcium input is normalized against aluminum (Ca/Al) to reflect the biogenic inputs of Ca from the swamp catchment located on an uplifted limestone mainly composed of CaCO3 rather than detrital Ca delivered through the river[1]. Interestingly, manganese records a second though smaller peak at this transition, reflecting a second change in the redox parameters in the system with an increase in oxygen that would be consistent with an hydrographic change to the system (Supplementary Figure S3).

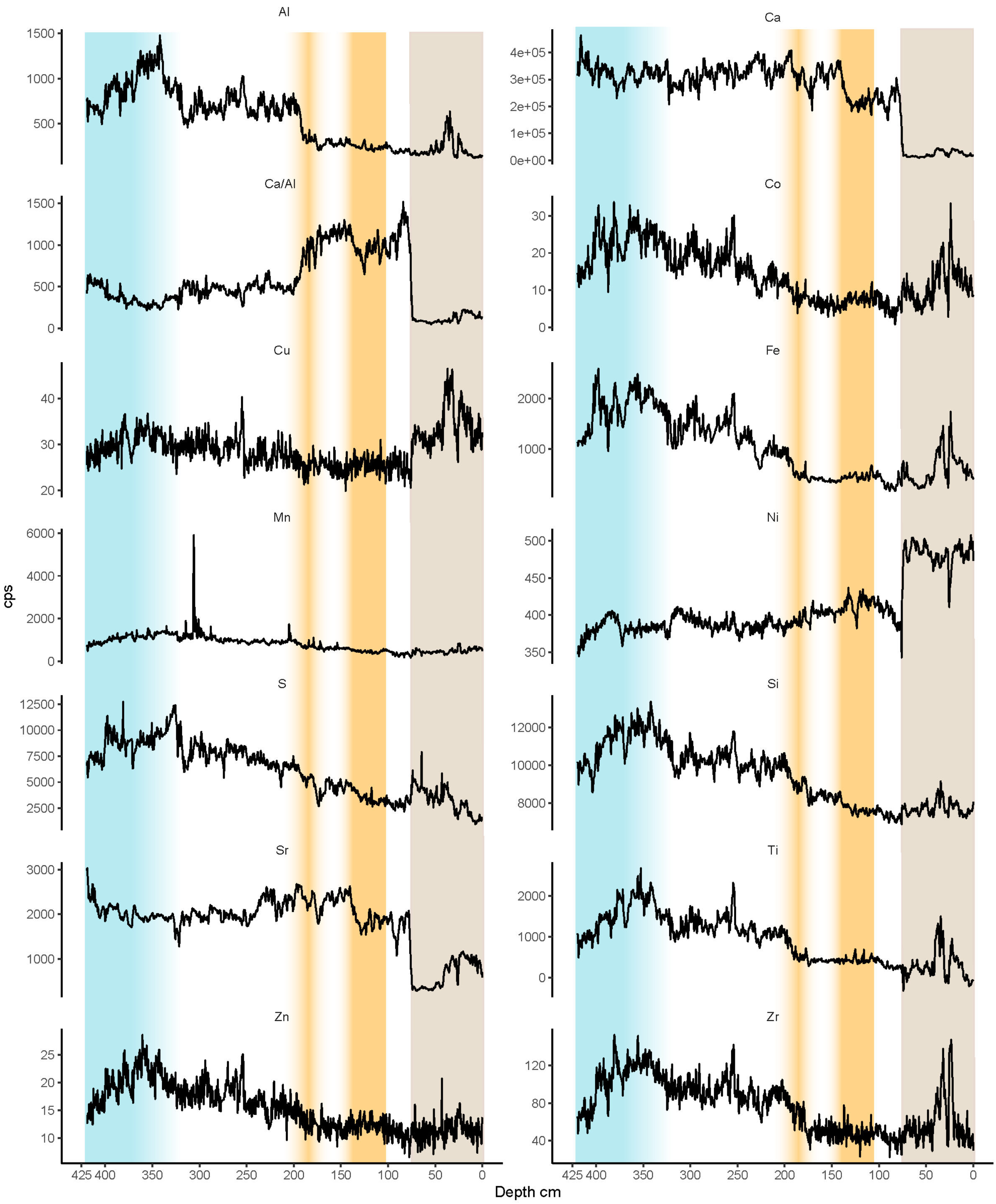

Supplementary figure S3. Downcore XRF elemental distribution in counts per seconds (cps). Light blue shading represents the marine period of the basin, yellow shadings represent periods of human occupation corresponding to the Lapita and Erueti phase in the archeological record, brown shading indicates the peat part of the core.

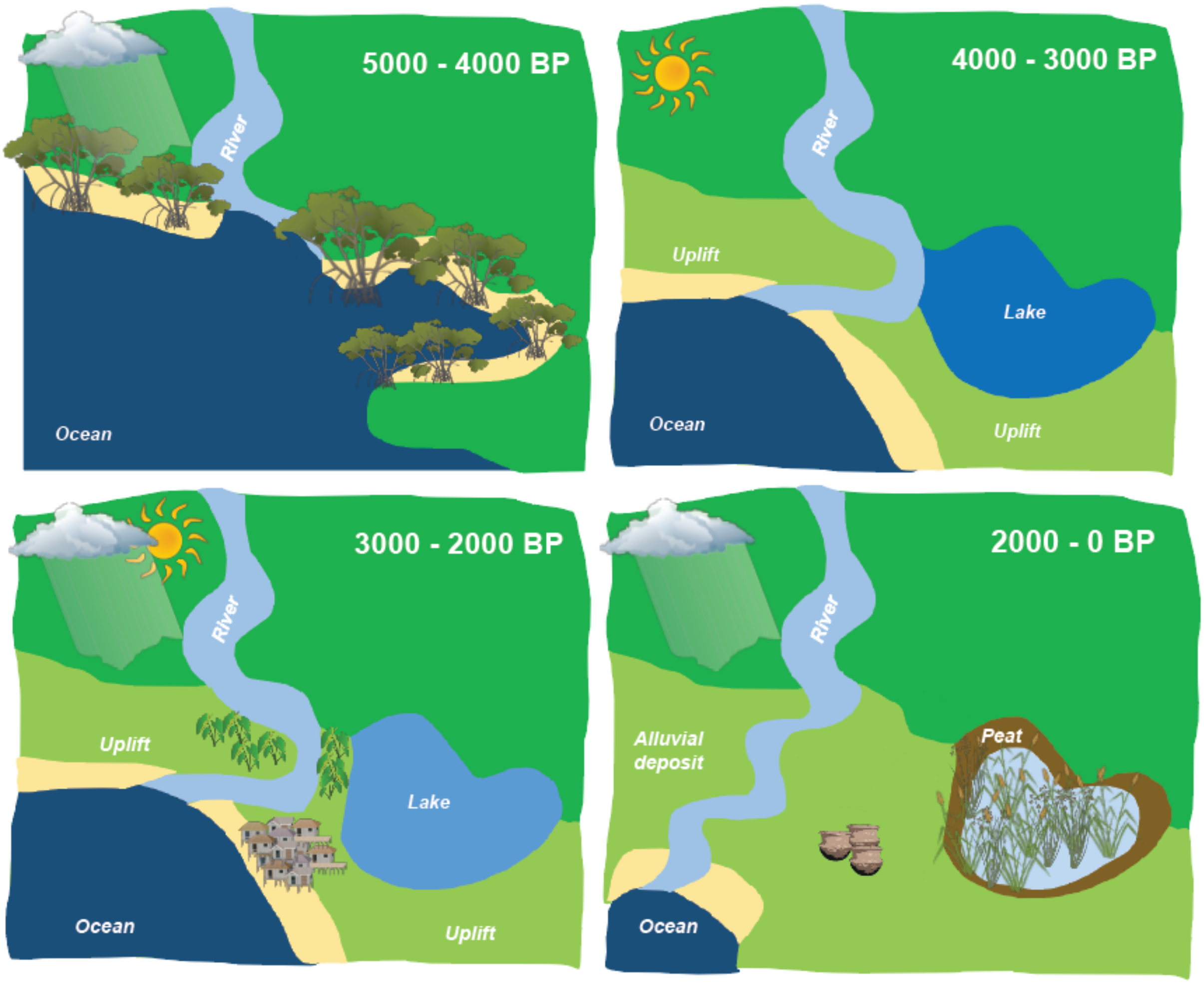

Supplementary figure S4. Graphical illustration of the landscape evolution at Emaotfer. The sedimentary basin used to be in a marine setting (4000-5000 BP) until it uplifted above sea level by 4000 BP. The system became a freshwater lake supplied in water and terrestrial material by the Teouma River (3000-4000 BP). The Teouma River disconnected from the Emaotfer system by 3000BP, turning it into a swamp. Peat started depositing by 2000BP.

Supplementary table S1. List of radiocarbon dates. Samples with $\delta^{13}C$ < 15 ‰ (in red), roots (*), and postbomb dates were excluded from the age model.

Sample#	**Material**	**Depth (cm)**	**^{14}C**	**1sigma**	**$\delta^{13}C$**
112215.1.1	plant remain	5	-1594.98	16.49535	-28.9154
112216.1.1	plant remain	17	-407.118	52.8852	-26.7007
112218.1.1	seeds	27	215.6113	54.34371	-25.9392
112217.1.1	plant remain	27	-881.863	16.93847	-27.7713
112219.1.1	wood	37	244.7261	17.48051	-26.742
132318.1.1	wood	45	2565.978	63.01346	-12.0122
112220.1.1	plant remain	47	-286.608	53.12796	-28.9753
132319.1.1	plant remain	52	2156.099	62.32595	-18.6946
112222.1.1	seeds	57	1742.86	18.37431	-26.9475
112221.1.1	charcoal	57	1772.818	18.0995	-22.6913
132321	charcoal	58	1859.4	22.3	-23.3
132321	seeds	58	2152	22.2	-18.5
112223.1.1	plant remain	66	2333.757	18.51597	-16.3938
132322	plant remain	68	2641.5	22.8	-14.4

101676.1.1	plant remain	71	263.7982	49.44817	-26.5995
101675.1.1	plant remain	71	377.8123	43.39346	-26.2
101677.1.1	plant remain	71	430.432	17.49433	-21.036
132323.1.1	organic matter	79	2965.436	62.56937	-8.7504
132324	organic matter	83	2814.9	22.7	-13.8
112224.1.1	plant remain	87	-200.651	17.48684	-24.3328
132325	organic matter	93	2741.7	22.6	-11.7
132326.1.1	organic matter	96	3025.461	65.8967	-7.27245
112225.1.1	plant remain	97	-354.338	17.68005	-23.974
112226.1.1	leaves	107	2131.366	59.64535	-31.1818
112227.1.1	uncertain	116	3016.177	18.82678	-15.6078
112228.1.1	plant remain	121	2519.753	18.70338	-23.3497
112229.1.1	plant remain	135	2397.87	18.59671	-27.3461
112230.1.1	plant remain	137	2320.664	18.39146	-27.1063
101678.1.1	uncertain	141	2813.47	48.30879	-19.4248
112231.1.1	plant remain	147	2479.525	25.56496	-21.1419
112232.1.1	plant remain	157	2514.084	18.66299	-27.9681

112234.1.1	plant remain	167	2463.097	18.65029	-27.8274
112235.1.1	plant remain	173	2621.23	20.2016	-26.9943
112237.1.1	plant remain	181	5768.658	19.55007	-28.5029
112238.1.1	plant remain	197	2932.635	23.50656	-23.5383
112239.1.1	plant remain	201	2781.083	59.43749	-29.3461
101679.1.1	plant remain	211	2894.336	47.88145	-26.727
112240.1.1	plant remain	217	3023.481	62.74917	-28.6933
112241.1.1	plant remain	227	3169.3	18.71432	-30.7218
112242.1.1	leaves	237	3034.711	19.38505	-29.2378
112243.1.1	plant remain	251	3131.815	21.78507	-25.5162
112244.1.1	plant remain	251	3142.045	18.4821	-28.8479
112245.1.1	plant remain	261	3895.671	19.63988	-23.0168
112246.1.1	leaves	271	3359.04	19.3245	-29.8783
101681.1.1	uncertain	281	3906.405	59.41965	-30.4982
101680.1.1	plant remain	281	3285.841	18.87053	-32.0953
112248.1.1	plant remain	291	3981.839	19.96592	-21.8751
112249.1.1	plant remain	307	3370.124	19.23137	-30.1708

112250.1.1	plant remain	317	3560.66	20.8267	-29.4368
132327	leaves	346	4834	23.2	5.2
101683.1.1	uncertain	351	4915.921	67.67333	-5.47945
101682.1.1	plant remain	351	6211.609	22.28236	-26.2335
132328.1.1	organic material	361	4377.013	68.71975	-22.0407
132329.1.1	plant remain	378	4114.594	66.40639	-28.0054
132330.1.1	leaves	391	5083.468	70.15887	-18.7501
132331.1.1	plant remain	421	3936.712	67.40213	-22.0576
101684.1.1	plant remain	425	3023.092	88.01014	-27.673

60

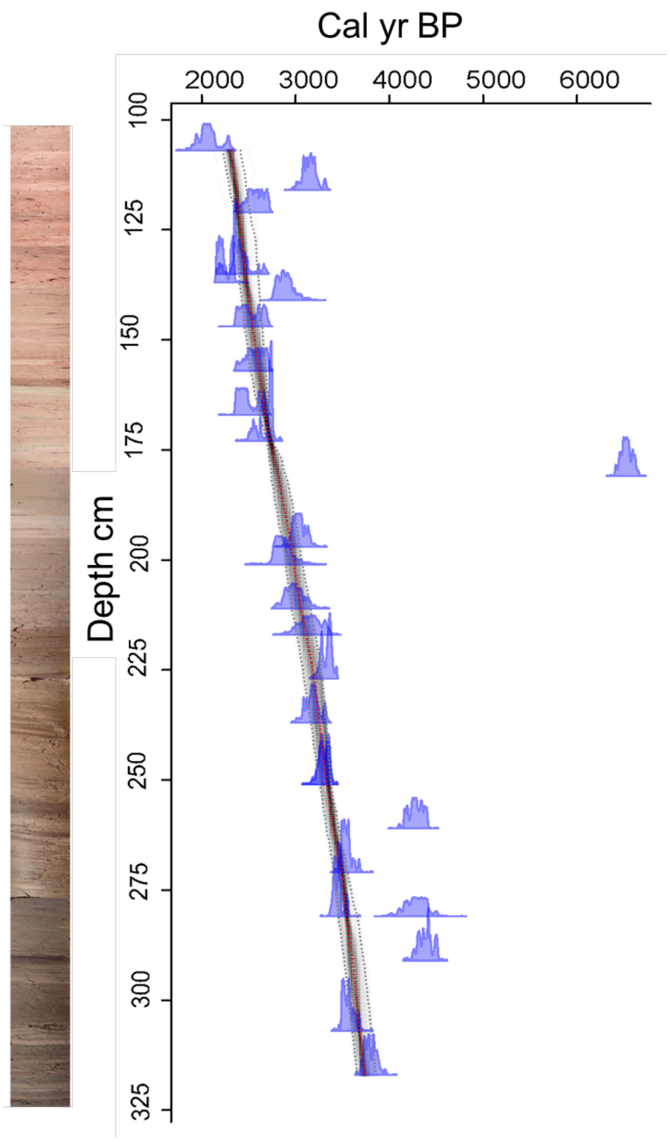

Supplementary figure S5. Additional separate detailed age-depth model from 107 cm to 307 cm, refining the period of first human presence and excluding the peat and marine phase of the core. Age model obtained with rbacon r package 3.0.0 (Blaauw and Christen, 2011). Although this separate age model does not differ much from the full chronology (average difference of 15 years), it was used for the interpretation of the record in this section.

Supplementary Information SI2 Sterols and palmitone

Measurements in selected ion monitoring mode (SIM) were carried out for quantification. External standards (supplementary table S2) were used to verify peak identity and quantification via external calibration curve. For analyses of sterol and stanol the initial column temperature program was 150°C (held 1 min), 1st ramp to 220°C at 40°C min-1, and 2nd ramp to 300°C at 3°C min-1 (held 5 min). For analyses of palmitone the initial column temperature program was 70°C (held 1. min) and a 1st ramp to 300°C at 20°C min-1 (held 15 min).

Supplementary table S2. List of sterols and ketone considered in this study with number of carbon atoms, origin, and selected ions (underlined the ions quantified), and standard details including producer, CAS number, and standard lot number.

Compound	**C atoms**	**Origin**	**Target m/z**	**Standard details**
Coprostanol	C27	Human feces	215, 355, 370	Sigma-Aldrich CAS 360-68-9 Lot 0000188007
Epicoprostanol	C27	Epimerization of coprostanol	215, 355, 370	Sigma-Aldrich CAS 516-92-7 Lot 127M4099V

Cholesterol	C27	Zoosterol	329, 368	Sigma-Aldrich CAS 57-88-5 Lot SLBR2606V
Cholestanol	C27	Zoosterol	370, 455	Avanti 80-97-7 Lot 700064P-5MG-J-011
Palmitone	C31	*Colocasia esculenta* schott	71, 239, 255	abcr GmbH, 16-Hentriacontanone; lot 1398514

Faecal molecules have been previously applied in sedimentary contexts to trace human presence and demography[2–7]. While coprostanol and epicoprostanol are not unique to humans, they are always associated with their presence on Pacific Islands as they are produced by pigs and other omnivores[8] that were introduced to the Remote Pacific islands by humans[9], strengthening their potential as tracers of human presence in this setting.

Ratios of faecal sterols are often reported in literature to discriminate against producers of molecules[8], but hold limited potential in this tropical setting given the disproportionate amount of cholestanol deriving from the environmental degradation of cholesterol[10]. Most of the ratios involve the use of cholestanol to correct for independent cholesterol degradation in the environment. However, the application of these ratios in tropical peats have not been tested. We tested the most used ratio of copr + epi / (copr+epi+cholestanol) (supplementary figure 6).

For this ratio, values above 3 are interpreted as faecal source and values above 9 are associated with humans or pigs[8]. Despite the ratio increasing during the periods of human occupation starting at 181 cm (indicate the average value in the human occupation period) the highest value of 6.8 is reached at 307 cm (3601-3810 BP). The low concentrations of cholestanol during the uplift phase could explain such peaks in the bottom of the core which cannot be interpreted as human presence given the low quantities of coprostanol and epicoprostanol at this time. The values of cholestanol compared to its main cholesterol source could also hint to other unidentified sterol sources. With degradation, sterols progressively lose double bonds, so the ratio of a sterol to its corresponding stanol could be an indication of down-core degradation of biomarkers in the swamp[11]. However, unconstrained factors can influence the results, *e.g.* trophic conditions[12] and taxonomic differences of living organisms, including the occurrence of stanols in various living organisms[13].

A constant minimum concentration of faecal sterols is present throughout the whole core (mean 0.1153 ± 0.091 μg/g), indicating inputs from other possible producers of faecal sterols that could be linked to microbial activity[14] or to the presence of other omnivores producing low quantities of faecal sterols (e.g. bats, birds, marine mammals)[15,16]. Constant quantities of palmitone are also present in the marine phase of the basin (mean 1.129 ± 0.4411 μg/g) indicating the possible production of this molecule by marine organisms. However, during the initial lake phase, palmitone is only present in low quantities (mean 0.584 ± 0.4380 μg/g) until 180 cm.

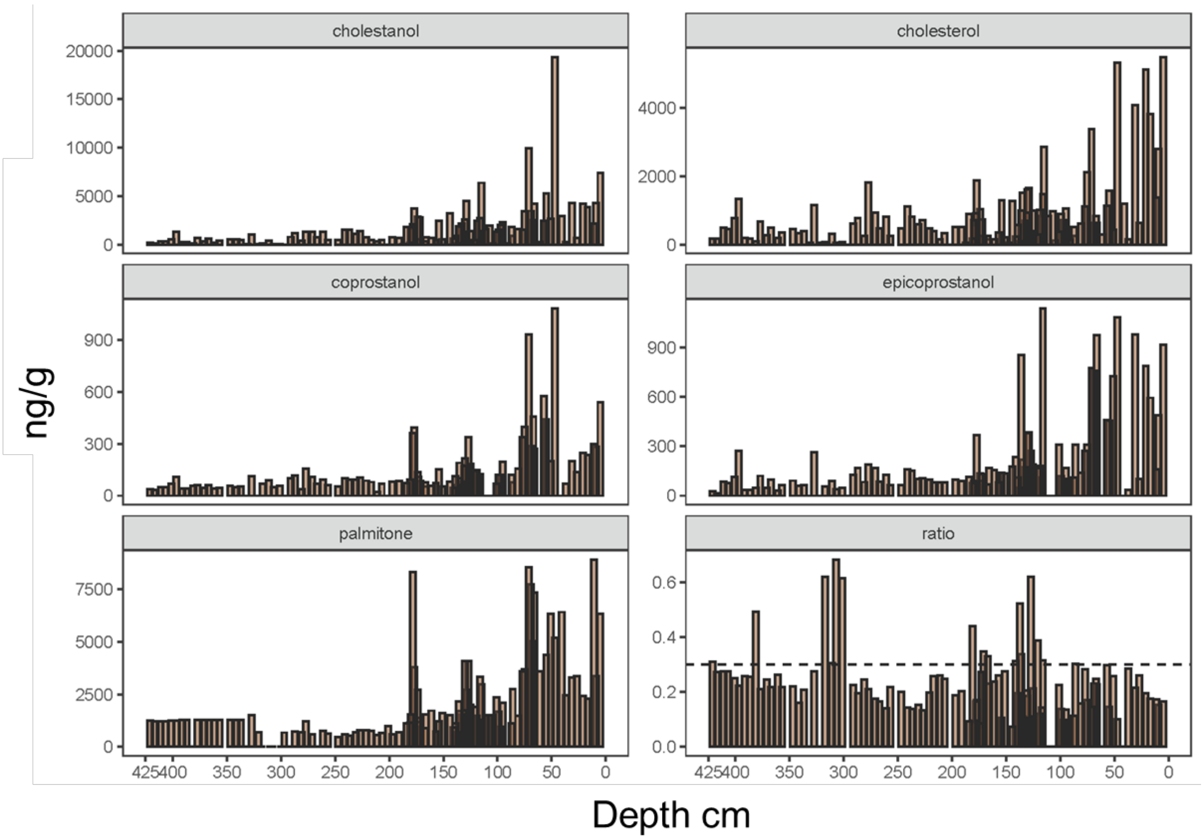

Supplementary figure S6. Detailed downcore distribution of all the sterols and stanols used in this study

Supplementary Information SI2. Assessing the robustness of leaf waxes dD in the Emaotfer record

In the Emaotfer sedimentary record, δ^2H of longer chain n-alkanoic acids (C26, C28, C30) covaried (Supplementary Figure S7). For the interpretation of hydroclimatic variations, we use the δ^2H C30 values, as this compound is most unambiguously associated with higher plants[17–19]. Lipid concentrations of modern plants collected in Vanuatu (Supplementary Figure S8) confirms that only few species produce n-C30 in the archipelago: The main producers are *Calophyllum inophyllum*, an indigenous tree which has the highest concentrations of C30, followed by the trees Tectona grandis, and *Burkella obovata*. Thus δ^2H of C30 can be considered a suitable marker for hydroclimatic changes captured by terrestrial vegetation in this context.

Besides changes in precipitation, δ^2H values can be affected by evapotranspiration that enhances isotopic values in dry conditions (enrichment), by changes in the vegetation source that can lead to different isotope fractionations[20], and by changes in the source and transport pathways of the rain/clouds[21–23].

Changes in plant community composition, such as the ones expected after land clearing for agriculture, can also introduce potential biological effects on the hydrogen isotopic composition of leaf waxes. Different plant species may have distinct isotopic fractionation patterns and physiological characteristics influencing δD composition. In order to exclude possible horticultural changes in vegetation as the main driver of the δ^2H signals, we calculated the relative offset between n-alkanoic acids, which can be expressed as epsilon Lipid 1–Lipid 2 values[24], that reinforce the signal of long chain-alkanoic acids in reconstructing hydroclimatic condition even in such variable context (Supplementary Figures S9 & S10).

In the Emaotfer core the stratigraphic changes characterising the three phases of the basin need to be considered carefully as the appearance of pink colouring in the sediment at 175 cm (2705-2796 BP) which intensify at 130 cm (2383-2579 BP), could be indicative of evaporative changes. These changes can also be accounted for by looking at the relative offset between n-alkanoic acids (Supplementary Figures S9 & S10). Epsilon values between different n-alkanoic acid pairs could change because of different producers with different water sources e.g., aquatic and terrestrial, or different producers with different biosynthetic fractionation. Biosynthetic fractionation is highly variable among species and does not clearly change with growth form.

When the swamp has a continuous flow of water through it and less evaporative enrichment, the source of water for aquatic plants represented by n-C22 and n-C24 (supplementary figure S10) tends to be δD depleted relative to the source water for terrestrial plants. Epsilon C30/22 values are positive, which is expected if n-C30 was primarily derived from trees and n-C22 was from a mix of terrestrial and aquatic sources (here the aquatic component makes the net δ^2H value for n-C22 lower).

When the swamp disconnects from the river, the source water δ^2H values converge, since both are affected by evaporative enrichment as well as precipitation isotopes. Nevertheless the "amount effect" and evaporative enrichment work in the same direction, thus δ^2H values can still be used to detect overall wetter/drier conditions, without quantitative inference. By comparison, the C28 δ^2H values have much bigger swings than C30, and this shows up in wildly fluctuating epsilon values for C28/30, C28/24, C28/22 (supplementary figure S10). This could be indicative of variable contributions from different plant sources that are not consistent over time, and makes the n-C28 less reliable than n-C30 for interpreting a primary hydroclimate signal. Nevertheless, n-C28 δ^2H values are positively correlated with n-C30 δ^2H values, indicating a main terrestrial source, and overall supporting the use of C30 δ^2H values as a wetter/drier indicator. Furthermore the comparison of epsilon values for C28/C30 between the dry and wet phase is non significant (ns) further supporting their use as hydroclimatic indicators (supplementary figure S9).

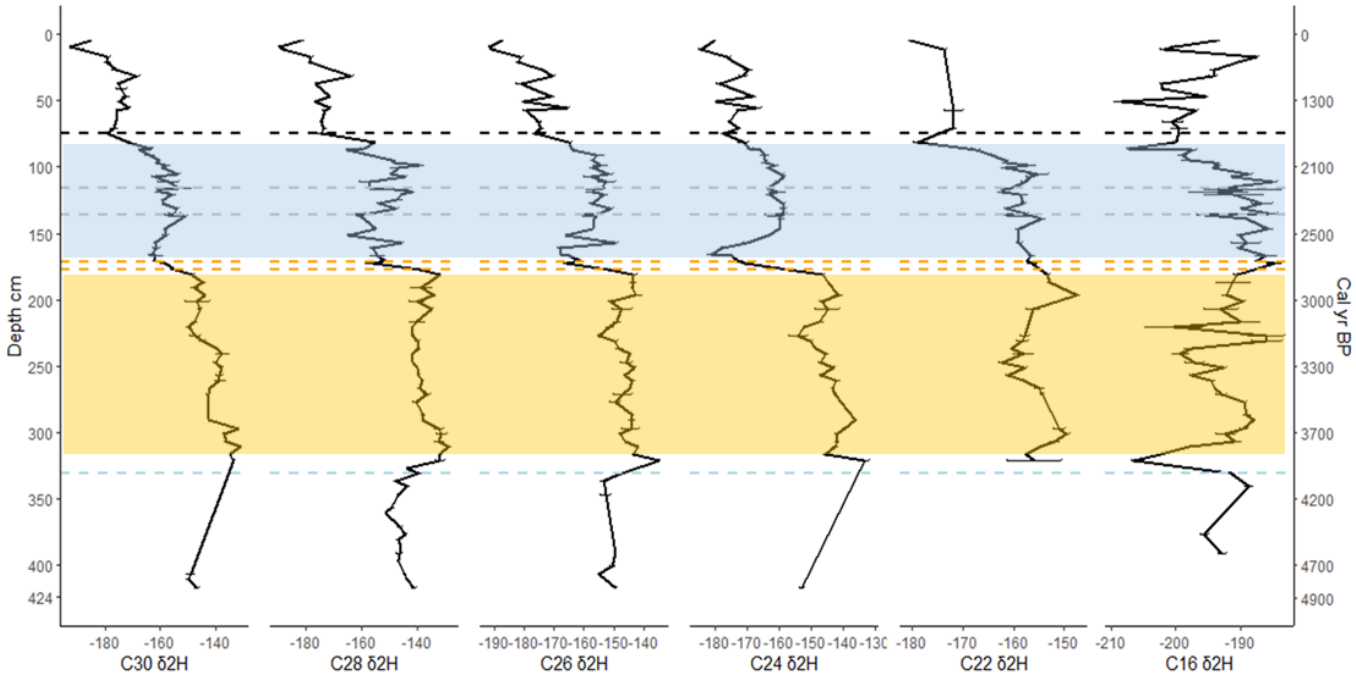

Supplementary figure S7. Downcore hydrogen isotopic composition of longer chain n-alkanoic acids in the Emaotfer record. The blue shading illustrates the wetter interval characterizing the time of initial settlement, while the yellow shading illustrates the preceding drier period. Dashed black lines indicate the onset of the peat, grey dashed lines correspond to the Erueti period and orange dashed to the Lapita period as identified by palmitone and fecal sterols.

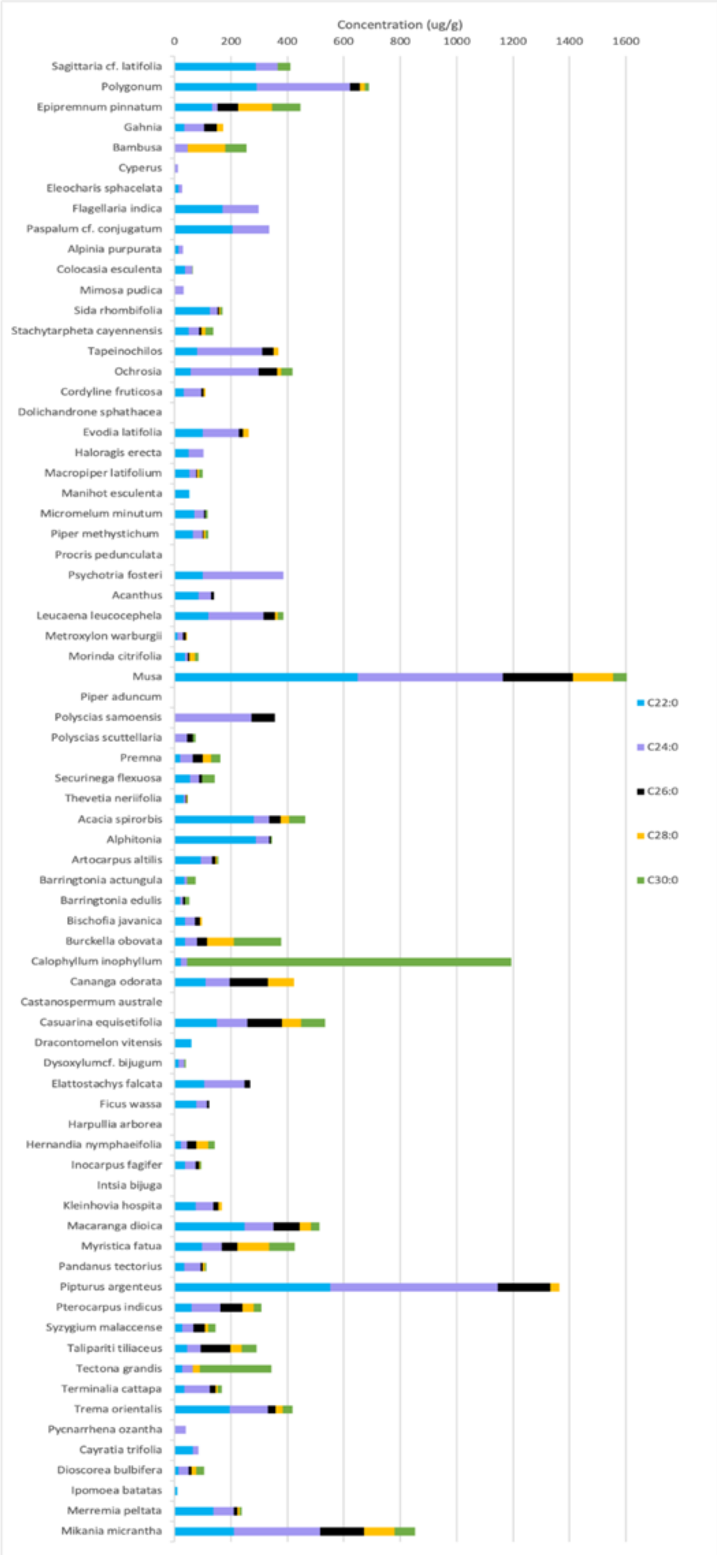

Supplementary figure S8. Fatty acid compilation from modern plants collected from Vanuatu. Details on plant collection and lipid extraction can be found in Krentscher et al. (2019). The fatty acid analysis was performed as described in this study.

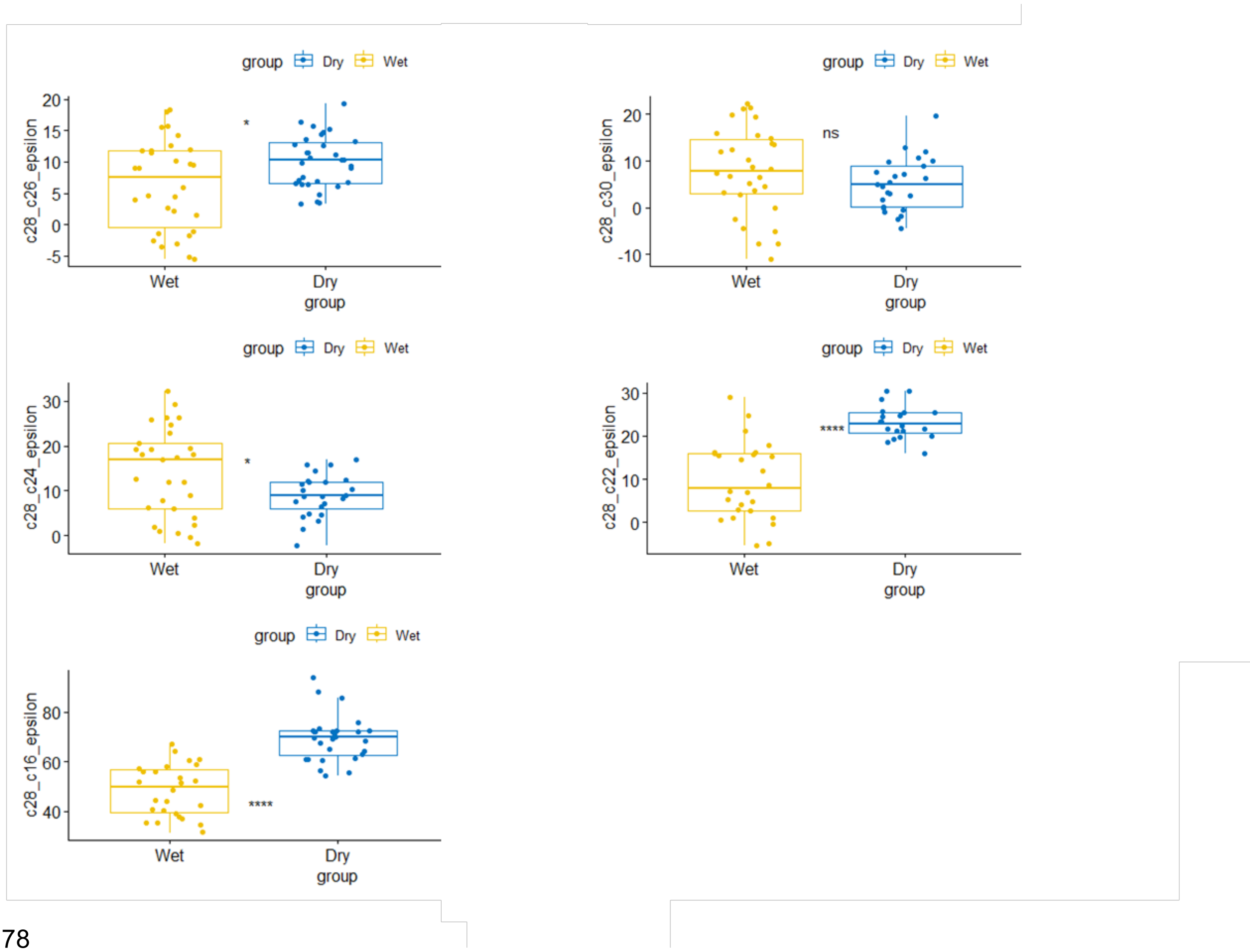

Supplementary figure S9. Box plots for the comparison between epsilon values in the dry (blue) and wet (yellow) phase defined in supplementary figure S7. The relative offset between n-alkanoic acids is shown as significant (*) or non significant (ns).

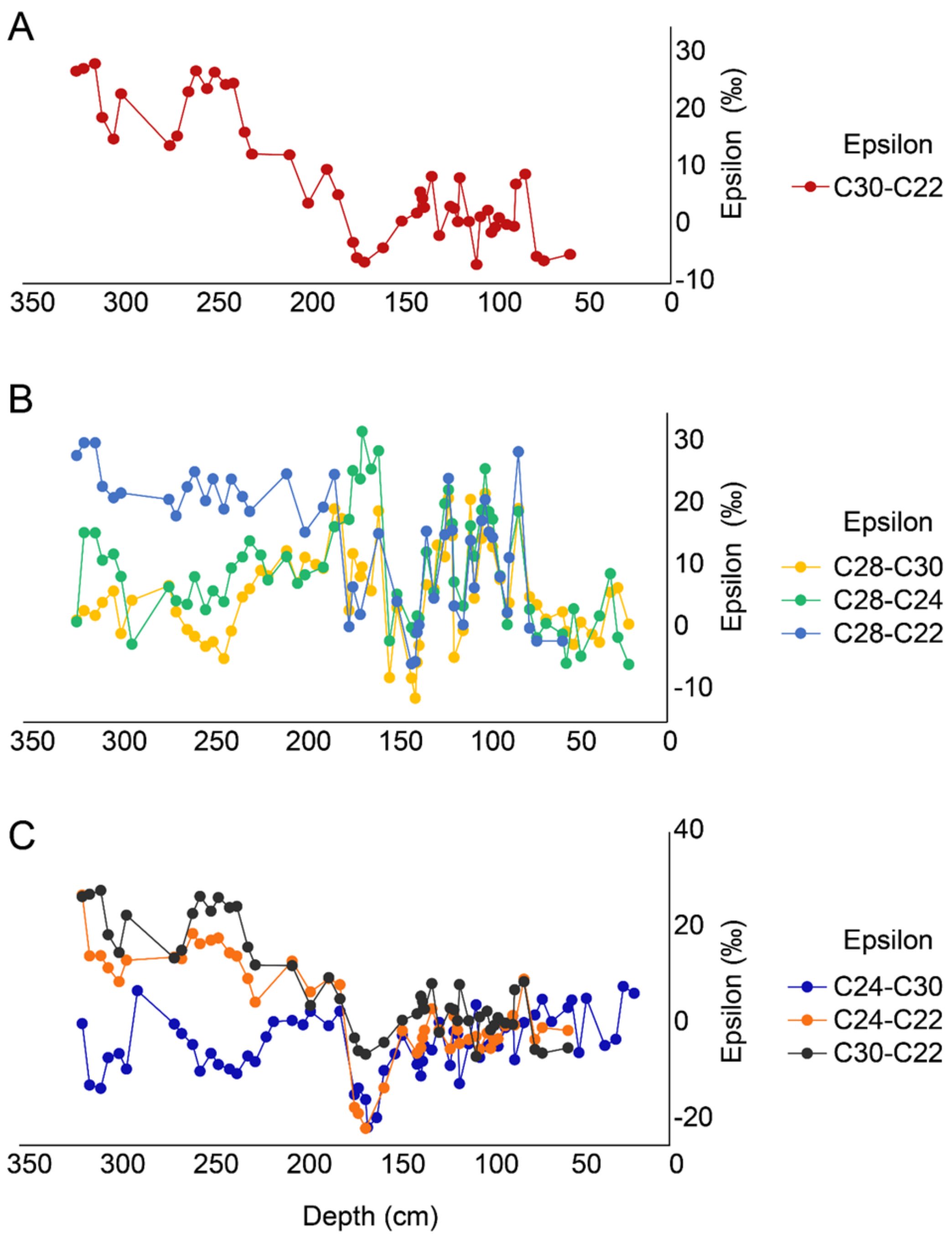

Supplementary figure S10. Downcore relative offset between n-alkanoic acids expressed as epsilon values. (A) Epsilon values for C30/C22 in red. (B) Comparison of C28/C30 (yellow), C28/C24 (blue), C28/C22 (light blue) epsilon values. (C) Comparison of C24/C30 (dark blue), C24/C22 (light blue), C30/C22 (light red) epsilon values.

References

1. Rothwell, R. G. & Croudace, I. w. Twenty Years of XRF Core Scanning Marine Sediments: What Do Geochemical Proxies Tell Us? in *Micro-XRF Studies of Sediment Cores: Applications of a non-destructive tool for the environmental sciences* (eds. Croudace, I. W. & Rothwell, R. G.) 25–102 (Springer Netherlands, 2015). doi:10.1007/978-94-017-9849-5_2.
2. D'Anjou, R. M., Bradley, R. S., Balascio, N. L. & Finkelstein, D. B. Climate impacts on human settlement and agricultural activities in northern Norway revealed through sediment biogeochemistry. *Proc. Natl. Acad. Sci. U.S.A.* **109**, 20332–20337 (2012).
3. Keenan, B. *et al.* Molecular evidence for human population change associated with climate events in the Maya lowlands. *Quaternary Science Reviews* **258**, 106904 (2021).
4. Raposeiro, P. M. *et al.* Climate change facilitated the early colonization of the Azores Archipelago during medieval times. *Proc. Natl. Acad. Sci. U.S.A.* **118**, e2108236118 (2021).
5. Sear, D. A. *et al.* Human settlement of East Polynesia earlier, incremental, and coincident with prolonged South Pacific drought. *Proc. Natl. Acad. Sci. U.S.A.* **117**, 8813–8819 (2020).
6. Shillito, L.-M. *et al.* Pre-Clovis occupation of the Americas identified by human fecal biomarkers in coprolites from Paisley Caves, Oregon. *Sci. Adv.* **6**, eaba6404 (2020).
7. White, A. J. *et al.* Fecal stanols show simultaneous flooding and seasonal precipitation change correlate with Cahokia's population decline. *Proc. Natl. Acad. Sci. U.S.A.* **116**, 5461–5466 (2019).

8. Prost, K., Birk, J. J., Lehndorff, E., Gerlach, R. & Amelung, W. Steroid Biomarkers Revisited – Improved Source Identification of Faecal Remains in Archaeological Soil Material. *PLoS ONE* **12**, e0164882 (2017).
9. Larson, G. *et al.* Phylogeny and ancient DNA of *Sus* provides insights into neolithic expansion in Island Southeast Asia and Oceania. *Proc. Natl. Acad. Sci. U.S.A.* **104**, 4834–4839 (2007).
10. Argiriadis, E. *et al.* Lake sediment fecal and biomass burning biomarkers provide direct evidence for prehistoric human-lit fires in New Zealand. *Sci Rep* **8**, 12113 (2018).
11. Meyers, P. A. & Ishiwatari, R. Lacustrine organic geochemistry—an overview of indicators of organic matter sources and diagenesis in lake sediments. *Organic Geochemistry* **20**, 867–900 (1993).
12. Mermoud, F., Gülaçar, F. O. & Buchs, A. 5α (H)-Cholestan-3α-ol in sediments: Characterization and geochemical significance. *Geochimica et Cosmochimica Acta* **49**, 459–462 (1985).
13. Nishimura, M. & Koyama, T. The occurrence of stanols in various living organisms and the behavior of sterols in contemporary sediments. *Geochimica et Cosmochimica Acta* **41**, 379–385 (1977).
14. Green, G., Skerratt, J. H., Leeming, R. & Nichols, P. D. Hydrocarbon and coprostanol levels in seawater, sea-ice algae and sediments near Davis station in eastern Antarctica: A regional survey and preliminary results for a field fuel spill experiment. *Marine Pollution Bulletin* **25**, 293–302 (1992).
15. Gallant, L. R. *et al.* A 4,300-year History of Dietary Changes in a Bat Roost Determined From a Tropical Guano Deposit. *Journal of Geophysical Research: Biogeosciences* **126**, e2020JG006026 (2021).

16. Venkatesan, M. I. & Santiago, C. A. Sterols in ocean sediments: novel tracers to examine habitats of cetaceans, pinnipeds, penguins and humans. *Mar. Biol.* **102**, 431–437 (1989).
17. Freeman, K. H. & Pancost, R. D. Biomarkers for Terrestrial Plants and Climate. in *Treatise on Geochemistry* 395–416 (Elsevier, 2014). doi:10.1016/B978-0-08-095975-7.01028-7.
18. Volkman, J., Johns, R., Gillan, F., Perry, G. & Bavor Jr, H. Microbial lipids of an intertidal sediment—I. Fatty acids and hydrocarbons. *Geochimica et cosmochimica acta* **44**, 1133–1143 (1980).
19. Van Bree, L. *et al.* Seasonal variability in the abundance and stable carbon-isotopic composition of lipid biomarkers in suspended particulate matter from a stratified equatorial lake (Lake Chala, Kenya/Tanzania): Implications for the sedimentary record. *Quaternary Science Reviews* **192**, 208–224 (2018).
20. Garcin, Y. *et al.* Hydrogen isotope ratios of lacustrine sedimentary n-alkanes as proxies of tropical African hydrology: Insights from a calibration transect across Cameroon. *Geochimica et Cosmochimica Acta* **79**, 106–126 (2012).
21. Aggarwal, P. K. *et al.* Proportions of convective and stratiform precipitation revealed in water isotope ratios. *Nature Geosci* **9**, 624–629 (2016).
22. Kurita, N. Water isotopic variability in response to mesoscale convective system over the tropical ocean. *Journal of Geophysical Research: Atmospheres* **118**, 10,376-10,390 (2013).
23. Risi, C. *et al.* Process-evaluation of tropospheric humidity simulated by general circulation models using water vapor isotopic observations: 2. Using isotopic diagnostics to understand the mid and upper tropospheric moist bias in the tropics and subtropics. *Journal of Geophysical Research: Atmospheres* **117**, (2012).

24. Ladd, S. N., Nelson, D. B., Schubert, C. J. & Dubois, N. Lipid compound classes display diverging hydrogen isotope responses in lakes along a nutrient gradient. *Geochimica et Cosmochimica Acta* **237**, 103–119 (2018).